

0280

50280

1133

ACTA UNIVERSITATIS SZEGEDIENSIS

ACTA PHYSICA ET CHEMICA

NEW SERIES

TOMUS XXXII

FASCICULI 1-4

AUSHAF 32 (1-4) (1986)

HU ISSN 0324-6523 Acta Univ. Szeged
HU ISSN 0001-6721 Acta Phys. et Chem.



1987 MAR 03

SZEGED, HUNGARIA
1986

ACTA UNIVERSITATIS SZEGEDIENSIS

ACTA PHYSICA ET CHEMICA

NOVA SERIES

TOMUS XXXII

FASCICULI 1—4.

AUSHAF 32 (1—4) (1986)

HU ISSN 0324—6523 Acta Univ. Szeged

HU ISSN 0001—6721 Acta Phys. et Chem

SZEGED, HUNGARIA

1986

Aduvantibus

M. BARTÓK, K. BURGER, L. CSÁNYI, J. CSÁSZÁR, P. FEJES,
P. HUHN, E. KAPUY, I. KETSKEMÉTY, F. SOLYMOSI, et F. SZÁNTÓ

Redigit

MIKLÓS BÁN

Edit

Facultas Scientiarum Universitatis Szegediensis de
Attila József nominata

Editionem curant

J. ANDOR, I. BÁRDI, Á. MOLNÁR, et Á. SÜLI

Nota

Acta Phys. et Chem. Szeged

Szerkeszti

BÁN MIKLÓS

A szerkesztő bizottság tagjai:

BARTÓK M., BURGER K., CSÁNYI L., CSÁSZÁR J., FEJES P.,
HUHN P., KAPUY E., KETSKEMÉTY I., SOLYMOSI F., és SZÁNTÓ F.

Kiadja

a József Attila Tudományegyetem Természettudományi Kara
(Szeged, Aradi vértanúk tere I.)

Szerkesztő bizottsági titkárok:

ANDOR J., BÁRDI I., MOLNÁR Á., és SÜLI Á.

Kiadványunk rövidítése:

Acta Phys et. Chem. Szeged

1s CORE-LEVEL SHIFTS IN Al CLUSTERS OF INCREASING SIZE

by

I. Gyémánt* and Zs. Varga

Department of Theoretical Physics, József Attila
University, P.O.B. 105, H-6701 Szeged, Hungary

(Received 10th October, 1986)

The Al 1s core-electron binding energy shifts have been calculated for Al₁₃ and Al₁₉ clusters by the MS X α method. The atom/cluster shifts calculated as the differences between the Slater transition-state energies for the 1s levels are 5.50 eV and 2.68 eV, for Al₁₃ and Al₁₉, respectively. These values are to be compared with the corresponding calculated X α Δ SCF results of 5.27 eV and 2.75 eV.

The determination of core-electron binding energy shifts has been attracting great interest and the significance of this problem is shown by the large number of papers published on this subject recently. The considerable amount of experimental and theoretical work has been motivated by the success of the use of soft X-rays (e.g. the Al K α line with an energy of 1487 eV and the Mg K α line with energy of 1254 eV) to study core levels with high resolution (~ 0.1 eV) [1-2]. It was early realized that the core-level energies depend on the chemical environment of the atom and are systematically several eV lower in conducting solids than in free atoms [3]. Measurements and calculations on the atom/molecule binding energy shifts have been performed for O₃, S₈, P₄, As₄ and Se_n [4-5]. It has been recognized that binding energy shifts reflect not only the ground-state charge distribution of the molecule, but also the energy associated with the rearrangement of the passive electrons in the final state. Results for F/F₂, Cl/Cl₂, Br/Br₂ and Na/Na₃ [6-7] show that without final-state effects the 1s binding energies would be higher in the molecule than in the atom, so that Δ SCF calculations, i.e. SCF calculations both for the initial and for the final state, have to be done.

The core-level binding energy is defined as:

$$E_c = E_f(n_c - 1) - E_i(n_c)$$

where $E_i(n_c)$ is the total energy in the initial state with n_c electrons, $E_f(n_c - 1)$ is that in the final state with $n_c - 1$ electrons, and n_c is the initial occupancy of the core level c . Nevertheless, in the $X\alpha$ approximation [8] the core-level binding energy can be approximated well by the Slater transition-state energy.

In this paper we present Δ SCF and transition-state results calculated with the MS $X\alpha$ method for Al 1s core-level atom/cluster shifts in clusters of 13 and of 19 Al atoms. The method was suggested by Slater [8] and was applied to calculate molecular ESCA spectra by Connolly et al. [9]. The geometry of the Al_{13} cluster corresponds to an Al atom and its 12 nearest neighbours in bulk Al of fcc structure with the lattice constant 404.3 pm. For Al_{19} the 2nd shell of 6 nearest neighbours has been included as well.

The muffin-tin version of the MS $X\alpha$ cluster MO method has been used [10]. The atomic region consists of atomic spheres 142.9 pm in radius around each of the atomic nuclei. The atomic spheres are enclosed in a sphere 428.8 pm in radius, the outer sphere, centred at the central atomic nucleus. The potential is spherically averaged inside the atomic spheres, as well as outside the outer sphere, and it is taken to be constant in the interatomic region, the region inside the outer sphere and outside the atomic spheres. The exchange parameter, α , has been chosen to be 0.7285 [11].

The 1s core-level binding energy for a free Al atom has been determined as the corresponding transition-state energy, which turned out to be -1577.23 eV, and we have used this value when calculating binding energy shifts. In Al clusters, the 1s level of the central Al atom has been studied, so that the symmetry of the cluster need not be changed on ionization, i.e. the O_h symmetry group could be used both in the initial and in the final states.

For Al_{13} the transition-state energy of the 1s level is -1571.73 eV and the difference in the total energies after and before the ionization gives 1571.96 eV. The corresponding values for an Al_{19} cluster are -1574.55 and 1574.48 eV, respectively.

The free-atom/cluster shift in a SCF calculation is given by the difference:

$$\Delta = E_{c,atom} - E_{c,cluster}$$

which can be approximated as the difference in the transition-state energies:

$$\delta = | \epsilon_{c,atom} | - | \epsilon_{c,cluster} |$$

For the Al_{13} cluster, $\delta = 5.5$ eV and $\Delta = 5.27$ eV have been obtained, i.e. transition-state energies can be used only to estimate total energy differences, considering that binding energies can be measured to an accuracy of 0.1 eV or better with XPS. Though no experimental and no theoretical results have been reported for Al clusters, both experimental and theoretical data are available for atom/metallic aluminium 1s core-level shifts. Experimental values for solid-state shifts are obtained either from direct simultaneous vapour-solid measurements or from comparison between calculated or measured atomic energies and separate solid-state measurements. The 1s binding energy 1568.8 eV of a free Al atom has been obtained semiempirically by Aksela et al. [12] in the following way.

The relativistic relaxed-orbital binding energy value 1567.87 eV of Huang et al. [13] was used as the starting value. The experimental free-atom binding energy value of 1568.4 eV was obtained from the thermochemical model [14] combined with X-ray data [15-16]. Because the deviations of the experimental free-atom binding energies from the *ab initio* calculations are systematic and slowly varying linear functions of Z in the series Ne, Na, Mg, Al, Si, P, S, Cl and Ar, Aksela et al. used linear interpolation for the correction by selecting the data on Ne and Ar as reference values.

An experimental solid-state $1s$ binding energy of 1558.2 eV relative to the Fermi level has been determined by Castle et al. [17]. This value has to be corrected by the work function of 4.28 eV [18] in order to obtain the binding energy relative to vacuum.

In this way, the experimental value of the atom/metal $1s$ binding energy shift for Al is 6.3 eV [12].

Various theoretical models, such as the "excited-atom approach" [19], the thermochemical model [20], etc., have been proposed. Spin-polarized density-functional conduction-electron screening calculations have been performed for core ionization by Nieminen and Puska [21] and Rantala [22]. The local-density exchange and correlation potential approximation of Gunnarsson and Lundquist [23] has been used in these self-consistent calculations, and for the "atom in jellium vacancy" model 6.3 eV [21] and 6.15 eV [22] have been obtained for the Al atom/solid $1s$ core-level binding energy shift, in good agreement with the experimental value.

Mali and Kanhere [24] presented results for the "atom in jellium vacancy" model with the exchange and correlation potential of Vashishta and Singwi [25], and they used transition-state theory instead of Δ SCF. However, their result for the $1s$ level turned out to be rather disappointing, 1.64 eV, too low compared with the experimental value of 6.3 eV. This large deviation is due to the inadequacy of the transition-state concept when the total energy-dependence on occupation number is different from that with an $X\alpha$ type exchange potential.

Taking into account the approximations used in the MS $X\alpha$ calculation, both the Δ SCF result of 5.27 eV and the transition-state result of 5.5 eV can be considered as good estimates and are in good agreement with the expected atom to solid trend of the binding energies.

However, the corresponding values for the Al_{19} cluster are 2.75 eV and 2.68 eV, respectively. These values are rather disappointing, since values higher than 5.27 eV would have been expected. This unexpected deviation is due to the artificial construction of the muffin-tin potential. The interatomic

region increases with increasing cluster size, and the proportions of the interatomic regions to the regions inside the atomic spheres are 0.519, 0.661 and 0.517 for Al_{13} , Al_{19} and Al_{43} , respectively. Therefore, the muffin-tin potentials are badly off in the case of Al_{19} and are expected to be realistic for Al_{13} and Al_{43} . Calculations for Al_{43} are now in progress, and results will be presented in a forthcoming paper.

REFERENCES

- [1] Siegbahn, K., C. Nordling, A. Fahlman, R. Nordberg, K. Hamrin, J. Hedman, G. Johansson, T. Bergmark, S.-E. Karlsson, I. Lindgren, B. Lindberg: ESCA-Atomic, Molecular and Solid State Structure Studied by Means of Electron Spectroscopy, North-Holland, 1967.
- [2] Siegbahn, K., C. Nordling, G. Johansson, J. Hedman, P. F. Hedén, K. Hamrin, U. Gelius, T. Bergmark, L.O. Werme, R. Manne, Y. Baer: ESCA Applied to Free Molecules, North Holland, 1969.
- [3] Shirley, D.A., R. L. Martin, S. P. Kowalczyk, F. R. McFeely, L. Ley: Phys. Rev. B15 544 (1977)
- [4] Banna, M.S.: Contemp. Phys: 25, 159. (1984)
- [5] Beck, D.R., R. J. Key, A. R. Slaughter, R. D. Mathews, M. S. Banna: Phys. Rev. A28, 2643 (1983)
- [6] Martin, R.L., E.R. Davidson: Phys. Rev. A16, 1341 (1977)
- [7] Martin, R.L., D. A. Shirley: Electron Spectroscopy: Theory, Techniques and Applications. Vol. 1. Ed. by C. R. Brundle, A.D. Baker, Academic Press, 1978. pp.76-117.
- [8] Slater, J.C.: The Self-Consistent Field for Molecules and Solids, Vol.4, McGraw-Hill, New York, 1974.
- [9] Connolly, J.W.D., H. Siegbahn, U. Gelius, C. Nordling: J. Chem. Phys. 58, 4265 (1973)
- [10] Liberman, D., J. R. Batra: Multiple Scattering Program Description. IBM Thomas J. Watson Research Center, New York, 1973.
- [11] Schwarz, K.: Phys. Rev. B5, 2466 (1972)
- [12] Aksela, S., R. Kumpulainen, H. Aksela, J. Väyrynen: Phys. Scripta 25, 45 (1982)
- [13] Huang, K.N., M. Aoyagi, M. Chen, B. Crasemann, H. Mark: Atomic Data and Nuclear Data Tables 18, 243 (1976)

- [14] Johansson, B., N. Mårtensson: Phys. Rev. B21, 4427 (1980)
- [15] Moore, C.E.: Atomic Energy Levels Circ. 467, Washington: Nat. Bur. stand (1971)
- [16] Bearden, J.A., Rev. Mod. Phys. 39, 78 (1967)
- [17] Castle, J.E., L. B. Hazell, R. D. Whitehead: J. Electron Spectrosc. 9, 247 (1975)
- [18] CRC Handbook of Chemistry and Physics, 58th Edition, CRC Press, Cleveland, 1977.
- [19] Watson, R.E., M.L. Perlman, J.F. Herbst: Phys. Rev. B13, 2358 (1976)
- [20] Steiner, P., S. Hüfner, N. Mårtensson, B. Johansson: Solid State Commun. 37, 73 (1981)
- [21] Nieminen, R.M., M.J. Puska: Phys. Rev. B25, 67 (1982)
- [22] Rantala, T.T.: Phys. Rev. B28, 3182, (1983)
- [23] Gunnarsson, O., B.I. Lundquist: Phys. Rev. B13, 4274 (1976)
- [24] Mali, S.J., D.G. Kanhere: phys. stat. sol. (b) 125, K143 (1984)
- [25] Vashishta, P., K.S. Singwi: Phys. Rev. B6, 875, (1972)

СДВИГИ 1s УРОВНЯ В КЛАСТЕРАХ АЛЮМИНИЯ С УВЕЛИЧЕНИЕМ
ИХ РАЗМЕРОВ

И.Н. Дьямант, Ж. Варга

Вычислены сдвиги энергии связи 1s электрона алюминия в кластерах алюминия Al_{13} и Al_{19} методом многократного рассеяния в $X\alpha$ приближения самосогласованного поля. Сдвиги 1s уровня, вычисленные разностями энергий переходных состояний, были 5.50 эВ в кластере Al_{13} и 2.68 эВ в Al_{19} . Эти величины сравнимы со сдвигами 5.27 эВ и 2.75 эВ вычисленными из разностей $X\alpha$ полной энергии.

ELECTRONIC ENERGY OF HEXAGONAL SITE SELF-INTERSTITIAL IMPURITY IN SI

by

G. Papp^{1*}, P. Bogusławski² and A. Baldereschi³

¹Department of Theoretical Physics, József Attila University,
Szeged, Aradi Vértanúk tere 1, HUNGARY

²Institute of Physics, Polish Academy of Sciences, Warsaw,
POLAND

³Institut de Physique Appliquée, Ecole Polytechnique Fédérale,
Lausanne, SWITZERLAND

Istituto di Fisica Teoretica, Università di Trieste, ITALY

(Received 12th October, 1986)

A point defect electronic structure calculation with the superlattice model in conjunction with the pseudopotential electronic structure calculation is described. The electronic energy variation of Si caused by self-interstitial impurity at the hexagonal site is investigated. Up to the bottom of the conduction band there are three main point defect-related states: a hyperdeep state at the bottom of the valence band, an s-like resonance near the middle of the valence band and a p_z -like bound state in the gap near the top of the valence band.

Introduction

Self-interstitial impurities in silicon have been studied extensively at different high-symmetry sites in the unit cell [1-5]. In this work we set out to describe the particular features of the electronic energy scheme of the hexagonal site (H) self-interstitial impurity.

Figure 1 shows a cube from the diamond structure. The points denoted by stars are those which have high symmetry and can be occupied by impurities. The letter A shows the host atom position; its point group is T_d . This point is an appropriate site for a substitutional impurity. The letter B denotes the bond centred atom position. If an impurity is situated at this point, it causes considerable distortion. Its point group is D_{3d} .

ISBN 963 481 610 X

Acta Phys. et Chem. Szeged 32 9-15 (1986)

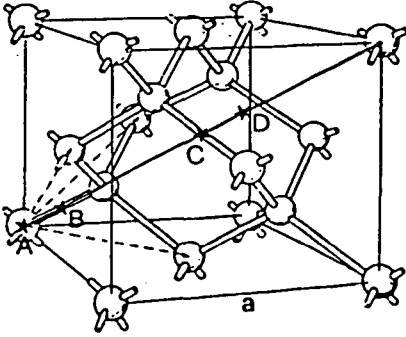


Figure 1: A cube from the diamond structure with highly symmetric points along the diagonal.

The letter C denotes the tetrahedral or antibonding site; its point group is also T_d . The letter D denotes the hexagonal site; its point group is D_{3d} . We examined the electronic structure of Si when the self-interstitial impurity is at the H site.

Model

Superlattice model: the host lattice is superimposed by another lattice which contains the impurities, and a cell is chosen in this lattice (host+impurity). If the impurity lattice constant is larger than the original one, then the impurities are distant from each other and the interactions between them are relatively small.

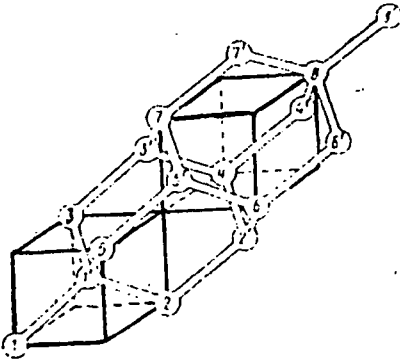


Figure 2: The atomic positions in the chosen cell.

The chosen cell is shown in Figure 2. We selected a FCC impurity lattice with doubled unit vectors (Si_{II}): in this case the cell contains sixteen host atoms and one impurity in the middle. This system retains translational symmetry, as the impurities are repeated periodically. Accordingly any method can be used which is appropriate for periodic systems. To calculate the electronic structure we used the self-consistent pseudopotential method.

Method

It is well known from elementary solid-state physics that there are numerous cases when it is not necessary to know the detailed description of the core electrons [6]: in these cases a pseudopotential can be used to simplify the calculations. The pseudopotential is determined for ions and it can be used as a starting potential for valence electronic structure calculations relating to the solid state.

Figure 3 shows the flow-chart of the procedure [7] leading to a self-consistent screening potential in response to a given structural model.

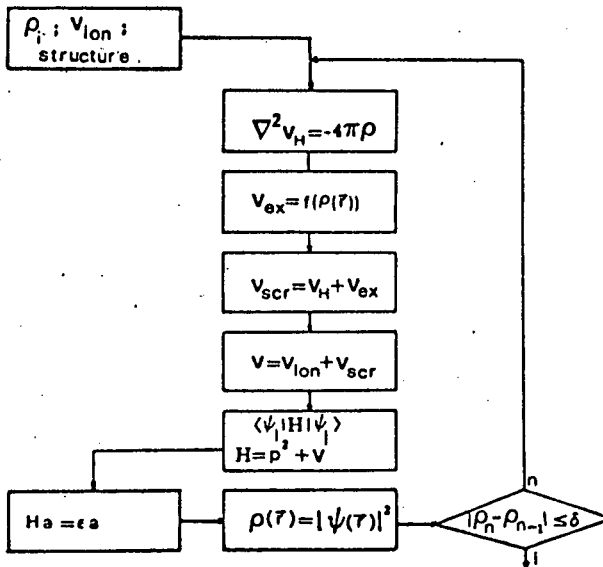


Figure 3: Flow-chart of the calculation

The following input system is required for a calculation:
The structure: the atomic positions in the coordinate system (as mentioned above, we used the FCC lattice).

V_{ion} : we used the soft-core Appelbaum-Hamann pseudopotential for Si^{4+} [8]. The Fourier transform of this potential is:

$$V(q) = 2/\Omega_{at} U(q) \exp(-q^2/(4\alpha)) \quad (1)$$

$$U(q) = -4\pi Z/q^2 + (\pi/\alpha)^{3/2} (v_1 + (3/(2\alpha) - q^2/(4\alpha^2))v_2) \quad (2)$$

where $v_1=3.042$, $v_2=-1.372$ and $\alpha=0.61$. If this potential is applied to the atomic sites, then the ionic potential can be written in the form:

$$V_{\text{ion}}(\vec{G}) = \sum_{\vec{G}} S(\vec{G}) V_{\text{ion}}^{\text{at}}(\vec{G}) \quad (3)$$

where

$$S(\vec{G}) = 1/M \sum_{\vec{R}} \exp(-i\vec{G}\vec{R}) \quad (4)$$

is the structure factor, which demands a knowledge of the atomic positions in the cell.

ρ_i : this is the initial value of the charge density. For pure Si, we chose the first component of the charge density to be equal to the number of valence electrons in the cell; the others were taken as 0. For the doped Si, the initial value of the charge was the self-consistent charge density of pure Si.

In the second step, we solved the Poisson equation to obtain the Hartree part of the potential.

For the exchange part of the potential, we used the $X\alpha$ approximation with $\alpha=0.76$. Summing up these two potentials, we obtained the screened electronic part of the potential.

Adding to this the ionic part, we found the pseudo-crystal-potential.

The pseudo-wavefunction was expanded on a plane wave basis:

$$\Psi^n(\vec{k}, \vec{r}) = \sum_{\vec{G}} a_{\vec{k}}^n(\vec{G}) \exp(i(\vec{k} + \vec{G})\vec{r}) \quad (5)$$

To obtain convergence results, the kinetic energy cutoff was about 100.68 eV (7.4 Ry) for pure Si, and this cutoff was used for Si_{II} also. About 700 plane waves were used for Si_{II}.

To calculate the charge density, an average is required over the Brillouin zone. We used the mean-value or representative-point technique [9] with $\vec{k}=2\pi a^{-1}(2/3, 0, 0)$.

Results

We first made test calculations on pure Si. Figures 4a and b show the electronic structure together with degenerations of Si_I and Si_{II}, respectively. The Si_{II} $E(\vec{k})$ curves contain 32 valence bands filled by two electrons. The shaded part of the figure is the band gap.

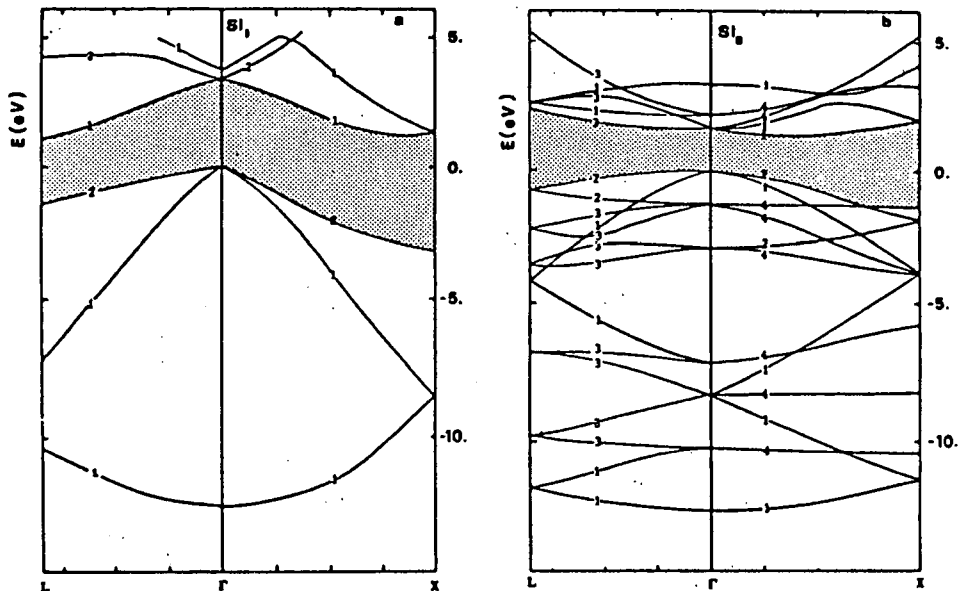


Figure 4: The $E(\vec{k})$ curves for Si with a two atomic unit cell (a) and with a sixteen atomic unit cell (b).

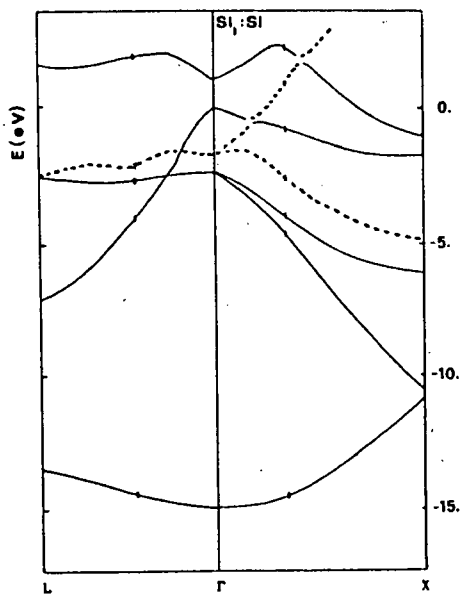


Figure 5: The electronic structure of Si with a self-interstitial impurity at the H site.

We studied the interactions between the impurities. We took a normal Si cell and placed a self-interstitial impurity at the hexagonal site. This gave the electronic structure shown in Fig. 5. The decreasing symmetry along the Γ -X axis caused the degeneration of the bands to decrease and an impurity-related band arose. Due to the interaction of the extra atoms, the dispersion of this band was very great. The band gap disappeared and a metallic like electronic structure resulted. The bottom of the valence band remained almost the same, but the top was changed drastically.

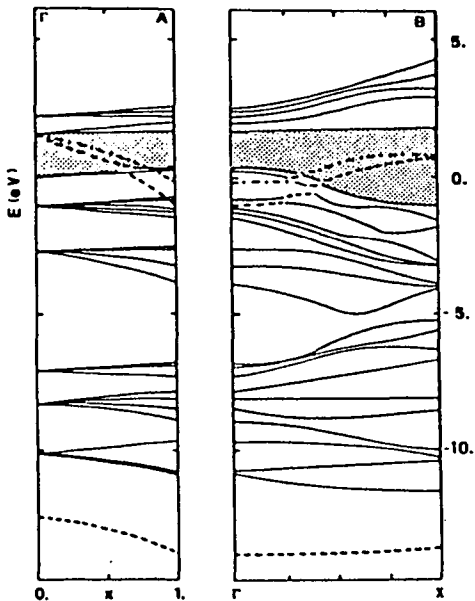


Figure 6: The electronic structure of $\text{Si}_{\text{II}} : \text{Si}_{\text{H}}$ along the Γ -X axis (B); the identification of the impurity-related states (A).

Figure 6B shows the band structure of $\text{Si}_{\text{II}} : \text{Si}_{\text{H}}$ along the Γ -X axis. The impurity-related states are indicated by dashed and dashed-dotted lines. There is an s-like hyperdeep level below the valence band, an s-like resonance in the valence band (dashed lines), and a p_z -like state near the top of the valence band (dashed-dotted line). The dispersion of the impurity-related bands is inherent in our method.

Figure 6A depicts one of the methods we used for the identification of impurity-related states. With the help of a switching parameter, we solved the eigenvalue problem of the following Hamiltonian:

$$H(x, \vec{r}) = p^2 / (2m) + V^p(\vec{r}) + x(V^d(\vec{r}) - V^p(\vec{r})) \quad (5)$$

where $V^p(\vec{r})$ and $V^d(\vec{r})$ are the pure and the doped Si crystal potentials, respectively; $0 \leq x \leq 1$. $x=0$ gives the pure Si, and $x=1$ gives the doped Si states. It can be seen from the left panel that at the hexagonal site two states are depressed from the conduction band and the results are the above-mentioned states.

REFERENCES

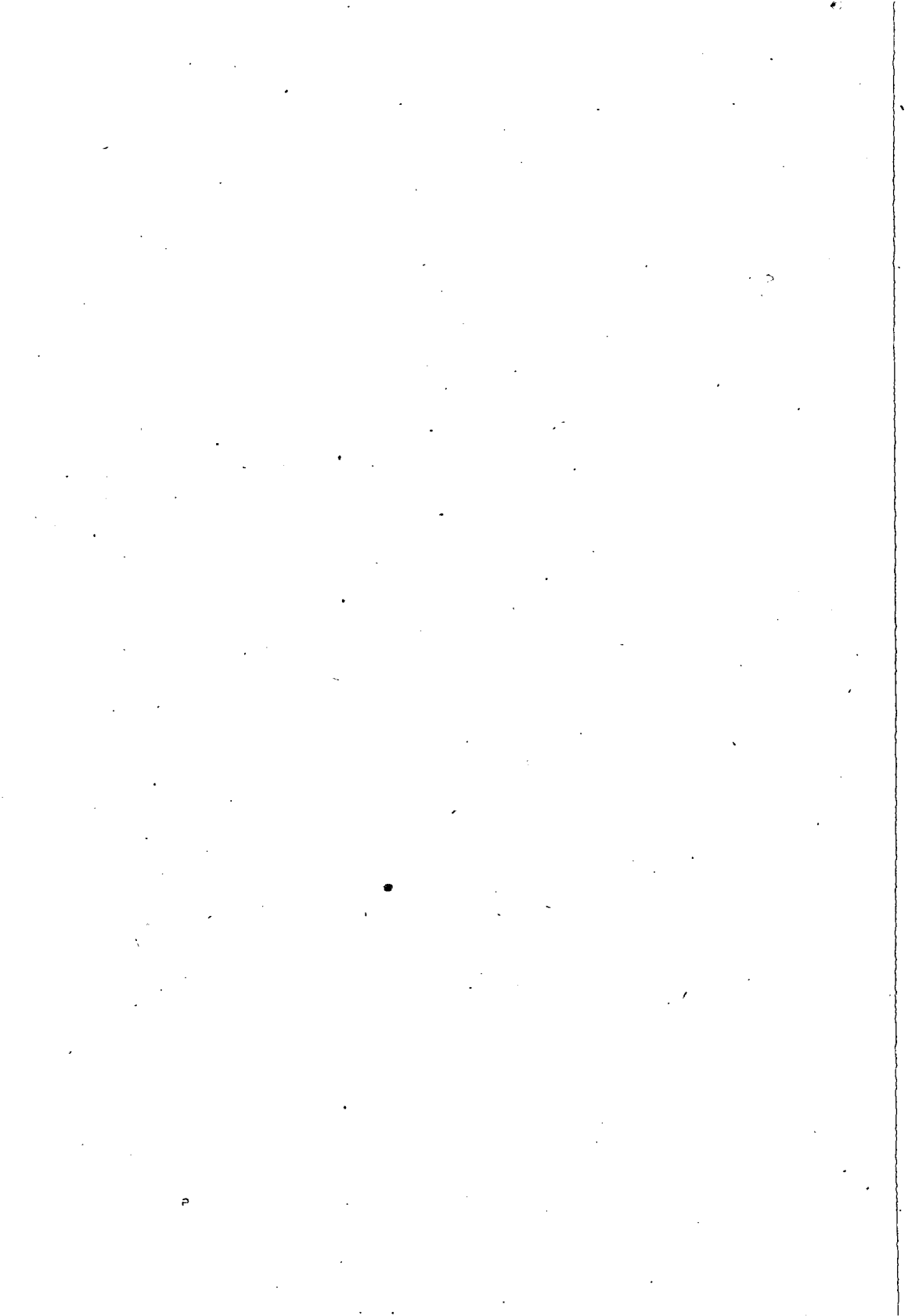
- [1] Boguslawski P., G. Papp, and A. Baldereschi: Solid State Comm. 52, 155 (1984)
- [2] Baraff G.A., M. Schlüter, and G. Allan: Phys.Rev.Lett. 50, 739 (1983); Physica, 116B, 76 (1983); Phys.Rev. B27, 1010 (1983)

- [3] Sankey O.F., and J.D. Dow: Phys.Rev. B27, 7641 (1983)
- [4] Pantelides S.T., I. Ivanov, M. Scheffler, and J.P. Vigneron : Physica 116B, 18 (1983) ; Vigneron J.P., M. Scheffler, and S.T. Pantelides: Physica 117B&118B, 137 (1983)
- [5] Bar-Yam Y., and J.D. Joannopoulos: Phys.Rev.Lett. 52, 1129 (1984)
- [6] Heine V., and D. Weaire: Solid State Physics 24, 249 (1970)
- [7] Louie S.G., M. Schlüter, J.R. Chelikowsky, and M.L. Cohen: Phys.Rev. B13, 1654 (1976)
- [8] Appelbaum J.A., and D.R. Hamann, Phys.Rev. B8, 1777 (1973)
- [9] Baldereschi A. : Phys. Rev. B7, 5212 (1973)

ЭЛЕКТРОННАЯ ЭНЕРГИЯ δ МЕЖДУУЗЛИЯ В КРЕМНИИ В ТОЧКЕ
ГЕКСАГОНАЛЫ

Г.Панп, П.Богуславски и А.Балдерески

Описываются расчеты электронной структуры точечного дефекта в модели суперрешетки методом псевдопотенциала. Исследуются изменения электронной структуры кремния за счет самомеждоузлия в точке гексагонали. До дна проводимости существуют три состояния связанные с точечным дефектом: гиперглубокое состояние на дне валентной зоны, δ типа резонанс близко к середине валентной зоны и связанное состояние типа p_z в запрещенной зоне, близко к потолку валентной зоны.



UV AND ^1H NMR SPECTRA AND CONFORMATIONS OF SUBSTITUTED N-BENZYLIDENEANILINES

By

J. Császár

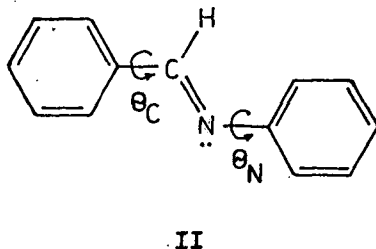
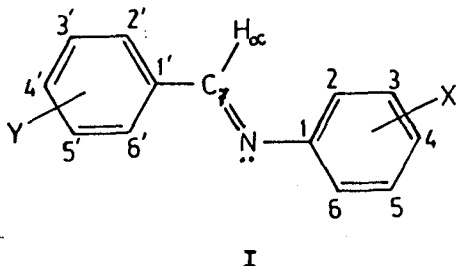
Institute of General and Physical Chemistry, József Attila
University, P.O.B. 105, H-6701 Szeged, Hungary

(Received 10th October, 1986)

The UV and ^1H NMR spectra of forty-three N-benzylidene-aniline derivatives were compared and the substituent effects on the molecular conformation were discussed on the basis of the twisting of the aromatic rings.

Introduction

The results of theoretical [1-7], crystallographic [8-12] and spectroscopic [7, 13-20] investigations on N-benzylidene-aniline (BA; I) and its substituted derivatives have been interpreted in terms of the twisting of the aromatic rings. UV absorption measurements revealed that the spectrum of BA differs markedly from those of the isoelectronic trans-stilbene and trans-azobenzene, and it can be concluded that the molecule is non-planar: the C-phenyl and the N-phenyl rings twist away from the other part of the molecule by different amounts ($8-14^\circ$ and $30-90^\circ$, respectively; II). One very interesting problem is



how substituent effects influence the conformation of the BA molecule and how this phenomenon is reflected in the different spectral characteristics.

In earlier papers [21-24] we discussed the UV and ^1H NMR spectra of the salicylideneaniline-type Schiff bases and, as a continuation of this work, we have now studied the spectral behaviour of the N-benzylideneanilines. In this work we report UV and ^1H NMR data.

Experimental

The Schiff bases were prepared by refluxing for about 15 min equimolar amounts of the appropriate aldehyde and aniline derivatives in methanol. After the solution was cooled, the crude crystalline products precipitated out; they were filtered off, washed with cool ethanol and ether, and recrystallized from 1:1 methanol-benzene. The analysis data and m.p.s were consistent with the literature data [2, 19, 42].

The UV spectra were recorded on a SPECORD UV-VIS spectrophotometer in the spectral range 200-500 nm, using spectroscopically pure solvents and 1.0 or 0.1 cm quartz cells. The ^1H NMR spectra were measured in CDCl_3 solution on a JEOL 60 MHz instrument at room temperature, using TMS as internal standard.

Results and Discussion

UV spectra

The electronic spectra of BA and its derivatives have already been reported [2-4, 7, 13-15, 18, 19, 25-27]. Several authors [8-12] have determined the molecular structures of these compounds by X-ray crystallography. Their absorption spectra may be characterized by three high-intensity bands, at around 230 (ν_1), 280 (ν_2) and 330 nm (ν_3). These bands can be assigned to the $\pi^* \leftarrow \pi$ transitions [2, 4, 7, 17, 18]; however, in some cases the ν_2 and ν_3 bands have a $\pi^* \leftarrow n$ character, too [7].

BA has an electronic structure similar to that of trans-stilbene, since the $-\text{CH}=\text{N}-$ and $-\text{C}=\text{C}-$ groups are isoelectronic [e.g. 2, 3, 14]. Stilbene gives an intense band at 295 nm and

a less intense one at 229 nm, while the spectrum of BA contains a shoulder at 315 nm and a band at 262 nm (Fig. 1). BROCKLEHURST

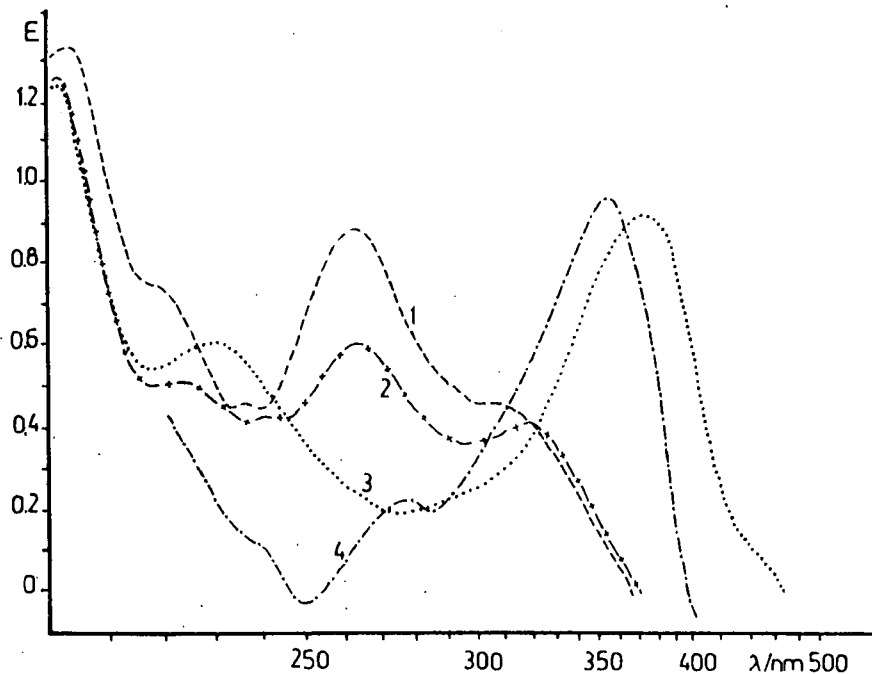


Fig.1. UV spectra of BA (1), $c=4.2 \cdot 10^{-4}$; the compound with $X=CH_3$ (2), $c=3.9 \cdot 10^{-4}$; the compound with $X=NO_2$ (3), $c=2.5 \cdot 10^{-4}$ mol/dm³, in methanol; BA in concentrated sulphuric acid (4), $c=3.1 \cdot 10^{-4}$ mol/dm³.

[14] suggested that the 315 nm band of BA corresponds to the 295 nm band of stilbene. The intensity of the 315 nm band is reduced compared to that of stilbene; this is due to the non-planarity of BA. The conformations of BA in solution and in the crystals are very similar, as demonstrated by the similarity of the absorption and reflection spectra [see e.g. ref. 30 and references therein].

From a comparison of the spectral data on several 4-X and 4'-Y derivatives (Table 1), it may be stated that the positions of the substitution and the character of the substituents play important roles. A Schiff base having an electron-donating group

Table 1
UV spectral data for BA and its 4- and 4'-derivatives

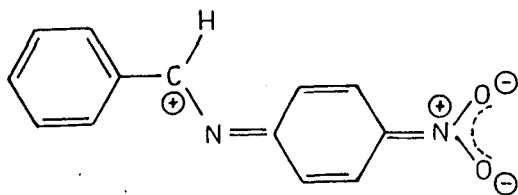
Y	X	Solvent [⊗]	nm and ε			ε _N
N(CH ₃) ₂	H ^{a)}	CH	238(15100)		356(39100)	
H	N(CH ₃) ₂	MA		252(20200)	374(18000)	30 ^{e)} , 34
OCH ₃	H ^{a)}	CH	222(18600)	280(19600)	315(12900)	43 ^{f)} , 38
H	OCH ₃ ^{b)}	EA	229(12900)	264(13100)	330(13300)	33 ^{e)} , 35
CH ₃	H ^{c)}	CH	227(14500)	268(18600)	319(8100)	48
H	CH ₃	MA	224(13200)	265(15050)	321(10050)	52 ^{f)} , 41
H ^{d)}	H	EA	236(10100)	263(16400)	315(6200)	44 ^{e)} , 55 ^{f)} , 54
H	F	MA	228(18500)	263(16600)	312(9550)	36
Cl	H	MA	225(14950)	266(18050)	317(10900)	38
H	Cl	MA	223(13800)	264(16500)	311(10500)	42 ^{e)} , 55 ^{f)} , 39
Br	H	MA	233(20050)	269(19050)	318(12500)	42
H	Br	MA	232(19950)	263(18400)	312(10600)	38 ^{e)} , 40
I	H	MA		266(21900)	324(13550)	
H	I	MA		262(20200)	310(11600)	40
NO ₂	H ^{d)}	CH	238(16250)	288(15600)	346(10200)	44 ^{f)}
H	NO ₂ ^{b)}	EA	243(17300)	290(3040)	380(16800)	~80

a) ref.[18], b) ref.[16], c) ref.[2], d) ref.[28], e) ref.[32], f) ref.[3];

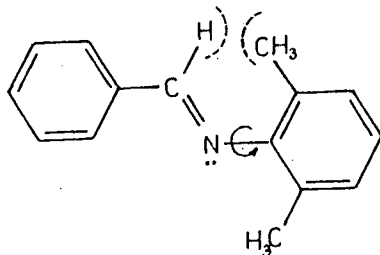
⊗ CH: cyclohexane, EA: ethyl alcohol, MA: methyl alcohol

in position 4 should absorb at longer wavelengths, in contrast to the base with the same substituent in position 4'; for an electron-withdrawing group the reverse tendency may be true.

The data in Table 1 show that for Y=H the ν_3/ν_2 or $\Delta\nu = \nu_3 - \nu_2$ values change regularly with the HAMMETT constant σ_p , but no appreciable tendency is to be observed for the halogen group. The very large bathochromic shift of the 4-NO₂ derivative may be interpreted in terms of the conjugation effect of the nitro group (III).



III



IV

With substituents in positions 2 or/and 2,6 a considerable steric factor exists (IV) and, as may be seen from Table 2, the

Table 2

UV data for some 2-, 2,6- and 2',4',6'-substituted derivatives

X,Y	Solvent*	nm and ϵ		
2-OCH ₃ ^{a)}	EA	246(11700)	~263	330(3850)
2-CH ₃ ^{b)}	CH	212(18100)	263(17100)	330(5900)
2-F ^{c)}	MA	225(17500)	261(17780)	310(8130)
2-Cl	MA	244(12400)	260(11350)	330(2800)
2-Br ^{c)}	MA	230(20100)	261(19700)	312(5620)
2-I	MA		256(22500)	321(4850)
2,6-(CH ₃) ₂ ^{b)}	CH	213(21300)	253(22300)	340(1800)
2',6'-(CH ₃) ₂	MA	212(22550)	267(20900)	313(2950)
2,4,6-(CH ₃) ₃	MA	213(19750)	258(20300)	322(3700)
2',4',6'-(CH ₃) ₃	CH	210(20800)	273(17500)	326(6300)

a) ref.[16], b) ref.[7], c) ref.[29], d) ref.[2]; * EA: ethyl alcohol, CH: cyclohexane, MA: methyl alcohol

absorbancy of the ν_3 peak decreases, while that of the ν_2 band increases; the change is due to the steric hindrance of planarity of the Schiff base molecules. The intensity of the ν_2 band decreases in the sequence $H \sim 2\text{-CH}_3 \sim 2,6\text{-(CH}_3)_2$. The effects of the substituents in position 2' are not so significant; the ϵ_2/ϵ_3 values for BA and the 2-CH_3 and $2,6\text{-(CH}_3)_2$ derivatives are 2.65, 2.90 and 12.40, respectively, while for the $2',4',6'\text{-(CH}_3)_3$ derivative it is only 2.78.

Interpretation of the spectra of the BA derivatives containing different substituents in positions 4,4' (Table 3) is

Table 3
UV data for Schiff bases containing different substituents
in 4 and 4'-positions

X	Y	Solvent*	nm and ϵ		
CH ₃	OCH ₃ ^{a)}	CH	221(18400)	280(20500)	322(14500)
OCH ₃	OCH ₃ ^{a)}	CH	221(20300)	280(22300)	330(17900)
CH ₃	NO ₂	MA	238(18600)	267(10480)	355(8350)
OCH ₃	NO ₂	MA	240(16750)	263(12600)	374(9550)
N(CH ₃) ₂	NO ₂ ^{b)}	MA		277(20400)	436(21000)
N(CH ₃) ₂	NO ₂ ^{b)}	CH		272(15200)	447(21300) ^{c)}
NO ₂	N(CH ₃) ₂ ^{b)}	MA	246(10400)	302(7700)	386(29350)
NO ₂	N(CH ₃) ₂ ^{b)}	CH	253(10900)	294(6560)	409(36800) ^{c)}

a) ref.[18], b) ref.[28], c) the corresponding indole derivatives;

* MA: methyl alcohol, CH: cyclohexane

complicated. The compounds with CH₃ or/and OCH₃ groups give spectra quite similar to those of the compounds listed in Table 1; our calculations indicate that these compounds have a twisted conformation with a twist angle of about 40-45°. A similar conclusion may be drawn for 4-methyl(methoxy)-N-(4-nitrobenzylidene)aniline. However, the spectrum of 4-dimethylamino-N-(4-nitrobenzylidene)aniline shows a close similarity [11] to those of the corresponding indole (Fig. 2) [28] and stilbene [11] ($\theta_C = 3.5^\circ$ and $\theta_N = 9.1^\circ$ [11]). 4-Nitro-N-(4-dimethylaminobenzylidene)aniline is not planar and a very highly conjugated system can be formed (V). The conjugation effect of the nitro group also plays an impor-

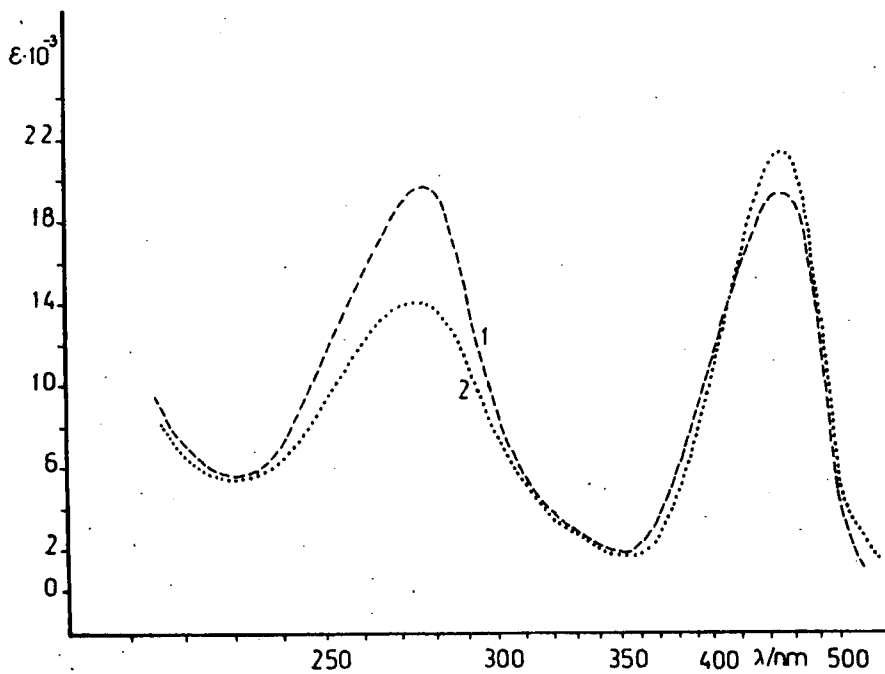
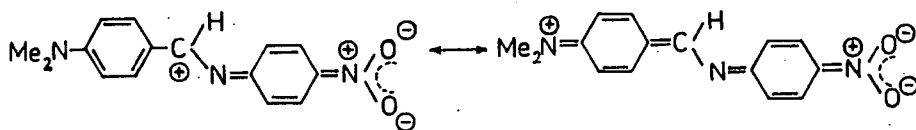
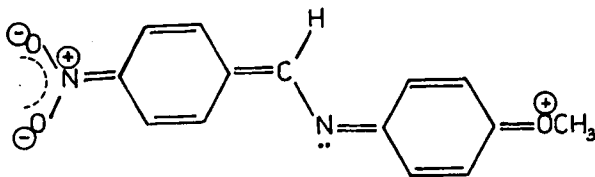


Fig.2. UV spectra of 4-dimethylamino-N-(4-nitrobenzylidene)-aniline (1) and of 5-dimethylamino-3,3-dimethyl-2-(p-nitrophenyl)-3H-indole (2) in cyclohexane.



V

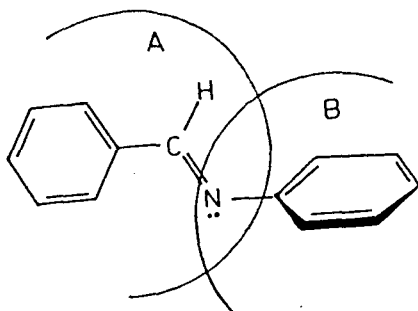
tant role in the formation of a quinoidal system (VI) in, for



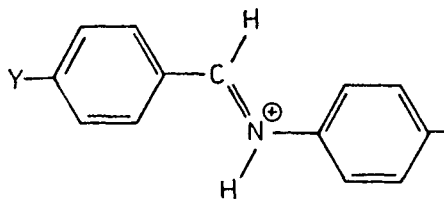
VI

example, 4-methoxy-N-(4-nitrobenzylidene)aniline, with a considerable bathochromic shift (see Table 3). SKRABAL et al. [28] concluded that the former compound is planar or nearly planar. On the other hand, the electron-acceptor CN derivative gives a spectrum quite similar to that of BA; the ring is rotated around the =N-C- bond. It seems that, with strong electron-donor and electron-acceptor groups in positions 4 and 4', the π -electron system extends to the whole molecule with a planar or nearly planar conformation.

If the molecule is planar, the π system extends over both of the phenyl rings and the azomethine group; the spectrum is similar to that of stilbene. However, if the molecule is non-planar, the spectrum should be a superposition of the spectra of two weakly interacting moieties A and B (VII) [17]. This is supported by the fact that the ν_3 band shifts to longer wavelengths as a result of N-phenyl substitution, while the ν_2 bands do not change their position. Thus, it is very probable that the ν_2 bands correspond to the C-phenyl ring, while the ν_3 bands correspond to the N-phenyl ring in the molecules.



VII



VIII

If the nitrogen lone-pair is localized by protonation [3, 14] or by nitron formation [3], the Schiff base favours the planar structure (VIII). In this case the lone-pair is not available for conjugation with the N-phenyl ring, and the spectrum of the protonated Schiff base is expected to be similar to that of trans-stilbene. According to theoretical calculations [28], the non-planar twisted conformation is favoured by ca. 8.4 kJ/mol; consequently, the -C=N- bond order is a function of the twist angle,

and a combination of the twisting and substituent effects should be taken into account in the explanation of the observed behaviour.

These Schiff bases show an anomalous solvent effect; the intensities of the ν_3 and ν_2 bands are higher in alcoholic and in benzene solution, respectively. This observation supports the conclusions that the molecules have a non-planar conformation and that the nitrogen lone-pair plays an important role in the spectra [14]. If hydrogen-bonding occurs between the lone-pair and the solvent molecule, the partial localization of the nitrogen doublet should favour a resonance contribution from the whole molecule.

If the spectra of the N-benzylideneanilines are measured in concentrated sulphuric acid, protonation takes place and the absorbancy of the ν_3 band ($\epsilon = 21000$; Fig. 3) increases considerable.

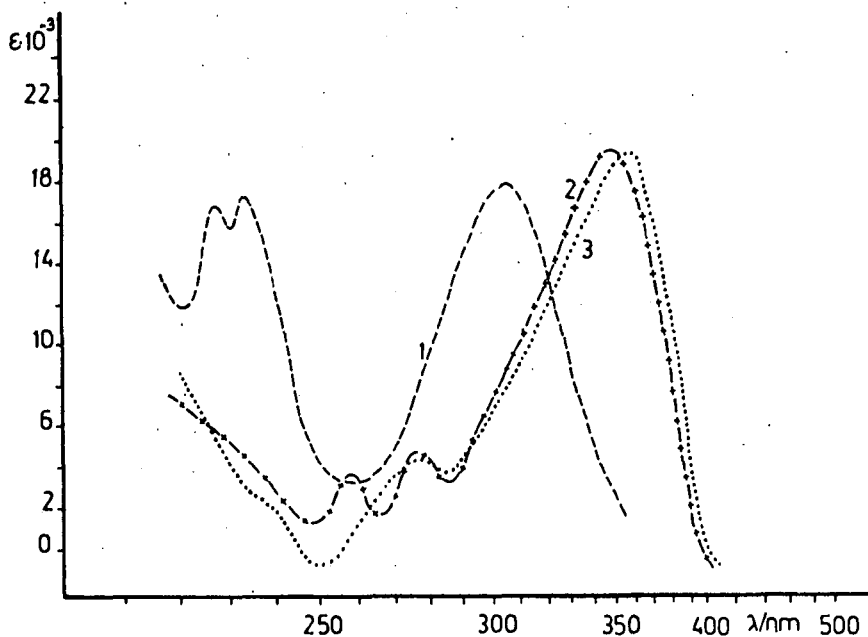


Fig.3. UV spectra of 3,3-dimethyl-2-phenylindolenine in hexane (1) and in concentrated sulphuric acid (2); BA in concentrated sulphuric acid (3).

rably. These spectra are similar to that of stilbene [28, 30]. In organic solvents the N-phenyl ring is twisted out of the plane

of the conjugate system consisting of the C-phenyl ring and the azomethine group, and the nitrogen lone-pair takes part in the π conjugation with the N-phenyl ring. In the protonated planar form the π conjugation extends over the whole molecule, but the nitrogen lone-pair does not take part in the π conjugation.

The degree of twisting of the N-phenyl ring around the =N-C-bond may be given in terms of the twist angle, θ_N , which can be estimated through the approximate formula $\cos^2 \theta_N = \epsilon / \epsilon_0$ [31]; ϵ and ϵ_0 are the molar extinctions of the base with non-planar (measured, e.g., in benzene) and planar (measured, e.g. in concentrated sulphuric acid) structures, respectively.

The θ_N values determined by different methods show considerable difference; e.g. for BA $\theta_N = 36^\circ$ [from UV data [32]], 46° (from HMO calculations [20]), 52° (from electron diffraction studies [5]), 55.2° (according to X-ray structural determination [10]), 65° (from NDDO calculation [6]). The different values make it necessary to calculate the twisting angles from data obtained by the same method under the same experimental conditions. It is interesting that the calculated θ_N values do not differ appreciably for the 4-X derivatives, except for the 4-NO₂ compound, and the substituents in the C-phenyl ring influence the twisting of the N-phenyl ring only slightly. The 2-CH₃ and 2,6-(CH₃)₂ compounds give twist angle $\theta_N = 48-55^\circ$ and $> 77^\circ$, respectively [34], corresponding to the high steric hindrance.

The twisted conformation of the N-benzylideneanilines is supported by several other experimental facts and theoretical considerations [35-39], as discussed, for instance, in [3].

Unfortunately, from UV spectral data alone it is not possible to conclude anything about the twisting of the C-phenyl ring.

¹H NMR spectra

Several studies have been reported [e.g. 40-49] on the effects of substituents on the NMR spectra of N-benzylideneanilines. In this work we discuss only the shift of the azomethine proton, H_α; the data are given in Tables 4-6.

The 4- or 4'-substituted compounds show an anomalous substituent effect on the H_α chemical shift. With an electron-withdra-

Table 4

Chemical shifts for H_α atom of the 4- or 4'-substituted
N-benzylideneanilines

Substituents	δH_α (ppm)	
	X = H	Y = H
$N(CH_3)_2$	8.27 ^{a)} , 8.35 ^{b)} , 8.31	8.54 ^{b)} , 8.47
OCH_3	8.35 ^{a)} , 8.40 ^{b)} , 8.38	8.45 ^{a)} , 8.50 ^{b)} , 8.51
CH_3	8.34 ^{a)} , 8.50 ^{b)} , 8.46	8.39 ^{a)} , 8.48 ^{b)} , 8.45
H		8.49 ^{b)} , 8.47
F	8.43	8.40 ^{c)} , 8.48
Cl	8.36 ^{a)} , 8.50 ^{b)} , 8.45	8.39 ^{a)} , 8.51 ^{b)} , 8.48
Br	8.36 ^{a)} , 8.44	8.40 ^{a)} , 8.44
I	8.45	8.36 ^{a)} , 8.37
NO_2	8.54 ^{a)} , 8.56 ^{b)} , 8.52	8.46 ^{b)} , 8.44

a) ref[35], b) ref.[38], c) ref.[40]

wing substituent in position 4, H_α exhibits an upfield shift with a positive ρ [from the plot of δH_α vs. σ_p] value, whereas with the same substituent in position 4', H_α exhibits a normal downfield shift with a negative ρ value. The H_α shifts for the 4'-derivatives correlate with the HAMMETT constants σ_p [40, 41, 45], while for the 4-derivatives there is no similar correlation [42]. In general, it may be said that the 4-X substituents have only weak effects on the H_α chemical shift [43] (Table 4).

The directions and magnitudes of the observed changes may be interpreted through the change in the twist angle θ_N [44], which is sensitive to the positions of substitution and to the properties of the substituents. With the strong electron-withdrawing NO_2 and the strong electron-donating $N(CH_3)_2$ groups, the picture is more complicated. The 4- NO_2 group generally results in an upfield shift, and the 4- $N(CH_3)_2$ group in a downfield shift. The 4- NO_2 group enhances the delocalization of the nitrogen lone-pair into the N-phenyl ring, while the $\pi \leftarrow n$ conjugation is accompanied by an increase in θ_N [7, 50]. This effect reduces the paramagnetic deshielding of the N-phenyl ring on the H_α , resulting in an upfield shift. The electron-donating $N(CH_3)_2$ group exerts a reverse effect [51].

AL-TAI et al. [43] suggested that the substitution effect of the 4-N(CH₃)₂ group could be ascribed to the predominance of the inductive effect over the resonance effect, because the N-benzylideneanilines generally assume a twisted conformation in solution, regardless of the substituents on them. However, AKABA et al. [45] proposed that the inverse substituent effect may arise primarily from the contribution of the paramagnetic deshielding effect of the N-phenyl ring on the H_α proton.

Alkyl substituents in position 4' or 4 do not influence the H_α chemical shift considerably (Table 4), but for the 2-CH₃, 2,6-(CH₃)₂ or 2'-CH₃ derivatives they give rise to up- or down-field shifts. The effects of methyl groups are not additive, which suggests that the upfield shift caused by the second or third methyl substitution might be due to the further distortion of the C-phenyl ring, but the inductive effect is also important. The increase in Θ_N on successive methyl substitution in the N-phenyl ring [44] will reduce the paramagnetic deshielding effect of the ring on H_α, resulting in an upfield shift; for the substitution on the C-phenyl ring the reverse effect may be observed. Table 5 shows that for 2-CH₃, 2,6-(CH₃)₂, 2,4,6-(CH₃)₃,

Table 5
Chemical shifts for H_α atom of N-benzylideneanilines substituted in 2-, 2,4-, 2,4,6-, 2',6'- or 2',4',6' positions

X	Y	δH_α (ppm)	X	Y	δH_α (ppm)
2-OCH ₃	H	8.45	2,4,6-(CH ₃) ₃	H	8.16 ^{a)}
2-CH ₃	H	8.27 ^{a)} 8.40 ^{b)}	2,6-(CH ₃) ₂	4-NO ₂	8.14 8.48
2-F	H	8.44	2,4,6-(CH ₃) ₃	4-NO ₂	8.28
2-Cl	H	8.47	H	2',6'-(CH ₃) ₂	8.25 ^{b)} 8.23
2-Br	H	8.38	H	2',4',6'-(CH ₃) ₃	8.72 ^{a)} 8.77
2-I	H	8.31	4-OCH ₃	2',4',6'-(CH ₃) ₃	8.75 ^{c)}
2-NO ₂	H	8.26	2,4,6-(CH ₃) ₃	4'-OCH ₃	8.09
2,6-(CH ₃) ₂	H	8.20			

a) ref.[41], b) ref.[37], c) ref.[36]

2',6'-(CH₃)₂ and 2',4',6'-(CH₃)₃ δH_α is 8.27, 8.20, 8.17, 8.25 and 8.72 ppm, respectively. In our calculations based on the UV

spectral data, ρ_N varies approximately in the same sequence. The $^{13}\text{C}_7\text{-H}$ coupling constant of BA (157.3 Hz) is increased to 158.5 and 159.6 Hz by methyl groups in positions 2 or 2,6, respectively, which indicates that methyl substitution on BA leads to an increase in the ρ character of the $\text{C}_7\text{-H}_\alpha$ bond, possibly through a decrease in the π electron density on C_7 [44].

If substituents are present on both the C-phenyl and N-phenyl rings, the interpretation of the observed H_α chemical shift (see Table 6) is ambiguous. 4-Dimethylamino-N-(4-nitrobenzylidene)aniline has a nearly planar conformation in solution [11, 28], with $\delta\text{H}_\alpha = 8.64$, while 4-nitro-N-(4-dimethylamino-benzylidene)aniline (according to our spectral studies) has a non-planar structure, with $\delta\text{H}_\alpha = 8.31$ [45] (Table 6). In

Table 6

Chemical shifts for H_α atom of 4,4'-substituted derivatives

X	Y	$\delta\text{H}_\alpha(\text{ppm})$	X	Y	$\delta\text{H}_\alpha(\text{ppm})$
Cl	Cl	8.25 ^{a)}	CH_3	NO_2	8.43 ^{c)}
OCH_3	OCH_3	8.37 ^{b)} 8.42	Cl	OCH_3	8.26 ^{b)} 8.31
$\text{N}(\text{CH}_3)_2$	$\text{N}(\text{CH}_3)_2$	8.40 ^{c)} 8.38	OCH_3	Cl	8.25 ^{b)} 8.28
NO_2	NO_2	8.55 ^{c)} 8.59	CH_3	NO_2	8.53 ^{b)}
CH_3	Cl	8.28 ^{a)} 8.26	OCH_3	NO_2	8.55 ^{b)}
Cl	NO_2	8.39 ^{a)}	$\text{N}(\text{CH}_3)_2$	NO_2	8.64 ^{c)}
			NO_2	$\text{N}(\text{CH}_3)_2$	8.31 ^{c)}

a) ref.[42], b) ref.[36], c) ref.[38]

general, ρ_N decreases from 4- NO_2 to 4- $\text{N}(\text{CH}_3)_2$, while the H_α chemical shift increases in this sequence. It is interesting that a NO_2 or $\text{N}(\text{CH}_3)_2$ group in position 4 results in an anomalous shift, regardless of the character of Y on the C-phenyl ring [45].

PAVLIK and PUTTEN [48] have published chemical shift data for BA and its methylated derivatives in concentrated sulphuric acid. The spectra are consistent with an ion in which the N-phenyl ring is twisted out of the molecular plane, and a limited positive charge delocalization into the C-phenyl ring is detectable.

References

- [1] Warren, C. H., G. Wettermark, K. Weiss: *J. Am. Chem. Soc.*, 93, 4658 (1971)
- [2] Smith, W. F.: *Tetrahedron*, 19, 445 (1963)
- [3] Minkin, V. I., Yu. A. Zhdanov, E. A. Megyantzeva, Yu. A. Ostroumov: *Tetrahedron*, 23, 3651 (1967)
- [4] Houlden, S. A., I. G. Csizmadia: *Tetrahedron*, 25, 1137 (1969)
- [5] Traetteberg, M., I. Hilmo, R. J. Abraham, S. Ljunggren: *J. Mol. Struct.*, 48, 395 (1978)
- [6] Hofmann, H.-J., F. Birnstock: *J. Mol. Struct.*, 44, 231 (1978)
- [7] Akaba, R., K. Tokumaru, T. Kobayashi: *Bull. Chem. Soc. Japan* 53, 1993 (1980) and references therein
- [8] Bürgi, H. B., J. D. Dunitz: *Chem. Comm.*, 472 (1969); *Helv. Chim. Acta*, 53, 1747 (1970)
- [9] Robertson, J. M., J. Woodward: *Proc. Roy. Soc., Ser. A*, 162, 568 (1937)
- [10] Bernstein, J.: *J. Chem. Soc., Perkin Trans.*, 2, 946 (1972)
- [11] Ezumi, K., H. Nakai, S. Sakata, K. Nishikida, M. Shiro, T. Kubota: *Chem. Lett.*, 1393 (1947)
- [12] Bernstein, J., I. Izak: *J. Chem. Soc., Perkin Trans.*, 2, 429 (1976)
- [13] Izmailskii, V. A., E. A. Smirnov: *Zh. Obshch. Khim.*, 26, 3042 (1956)
- [14] Brocklehurst, P.: *Tetrahedron*, 18, 299 (1962)
- [15] Favini, G., A. Gamba: *J. Chim. Phys.*, 62, 995 (1965)
- [16] Ebara, N.: *Bull. Chem. Soc. Japan*, 33, 534 (1960)
- [17] Ebara, N.: *Bull. Chem. Soc. Japan*, 34, 1151 (1961)
- [18] El-Bayoumi, M. A., M. El-Aasser, F. Abdel-Halim: *J. Am. Chem. Soc.*, 93, 586 (1971)
- [19] Klasing, L., B. Ruscio, G. Heinrich, H. Güsten: *Z. Naturforsch.*, 32 B, 1291 (1977)
- [20] Goetz, H., F. Marschner, H. Jude: *Tetrahedron*, 30, 1133 (1974)
- [21] Császár, J., J. Balog, A. Makáry: *Acta Phys. Chem., Szeged*, 24, 473 (1978)
- [22] Császár, J.: *Acta Phys. Chem., Szeged*, 25, 137 (1979)

- [23] Császár, J.: *Acta Phys. Chem.*, Szeged, 27, 47 (1981)
- [24] Császár, J.: *Acta Phys. Chem.*, Szeged, 39, 133 (1983)
- [25] Wiegand, C., E. Merkel: *Liebigs Ann. Chem.*, 550, 175 (1942)
- [26] El-Aasser, M., F. Abdel-Halim, M. A. El-Bayoumi: *J. Am. Chem. Soc.*, 93, 590 (1971)
- [27] Favini, G., D. Pitea, F. Zuccarello: *J. Chim. Phys.*, 69, 9, (1972)
- [28] Skrabal, P., J. Steiger, H. Zollinger: *Helv. Chim. Acta*, 58, 800 (1975)
- [29] Favini, G., J. R. Bellobono: *Gazz. Chim. Ital.*, 96, 1423 (1966)
- [30] Haselbach, E., E. Heilbronner: *Helv. Chim. Acta*, 51, 16 (1968)
- [31] Braude, E. A., F. Sondheimer: *J. Chem. Soc.*, 3754 (1955)
- [32] Kraszovickij, B. M., B. M. Bolomin, R. N. Nurmahatmetev: *Zh. Obsch. Khim.*, 34, 3786 (1964)
- [33] Bally, T., E. Haselbach, S. Lanylova, F. Marschner, M. Rossi: *Helv. Chim. Acta*, 59, 486 (1976)
- [34] Akaba, R., K. Tokumaru, T. Kobayashi, C. Utsunomiya: *Bull. Chem. Soc. Japan*, 53, 2006 (1980)
- [35] Kiprianov, A. I., V. A. Shrubovich: *Zh. Obsch. Khim.*, 29, 1290 (1959)
- [36] Minkin, V. I., O. A. Osipov, V. A. Kogan: *Dokl. Akad. Nauk. SSSR*, 145, 236 (1962)
- [37] Fischer, E., Y. Frei: *J. Chem. Phys.*, 27, 808 (1957)
- [38] Anderson, D. G., G. Wettermark: *J. Am. Chem. Soc.*, 87, 1433 (1965)
- [39] Minkin, V. I., E. A. Medyantzeva: *Zh. Obsch. Khim.*, 35, 1956 (1965)
- [40] Tabei, K., E. Saitou: *Bull. Chem. Soc. Japan*, 42, 1440 (1969)
- [41] Inamoto, I., K. Kushida, S. Masuda, H. Ohta, S. Satoh, Y. Tamura, K. Tokumaru, K. Tori, M. Yoshida: *Tetrahedron Letts.*, 1617 (1974)
- [42] Echevarria, A., J. Miller, M. G. Nascimento: *Magn. Res. in Chemistry*, 23, 809 (1985)
- [43] Al-Tai, A. S., D. M. Hall, A. R. Mears: *J. Chem. Soc.*, Perkin, 133 (1976)

- [44] Akaba, R., H. Sakuragi, K. Tokumaru: Bull. Chem. Soc. Japan, 58, 301 (1985)
- [45] Akaba, R., H. Sakuragi, K. Tokumaru: Bull. Chem. Soc. Japan, 58, 1711 (1985)
- [46] Inamoto, N., S. Masuda, K. Tokumaru, M. Yoshida: Tetrahedron Letters, 43, 3697 (1975)
- [47] Sandhu, J. S., D. Mago: Tetrahedron Letters, 13, 1091 (1975)
- [48] Pavlik, J. W., A. van Putten: Tetrahedron, 27, 3301 (1971)
- [49] Gil, V. M. S., M. E. L. Saraiva: Tetrahedron, 27, 1309 (1971)
- [50] Akaba, R., K. Tokumaru, T. Kobayashi, C. Utsunomiya: Bull. Chem. Soc. Japan, 53, 2002 (1980)
- [51] Steiger, J., H. Zollinger: Helv. Chim. Acta, 58, 800 (1975)

УФ и ^1H ЯМР СПЕКТРЫ И КОНФОРМАЦИИ ЗАМЕЩЕННЫХ
N-БЕНЗИЛИДЕНАНИЛИНОВ

И. Часар

Изучены спектры протонного ядерного магнитного резонанса и в ультрафиолетовой области сорока трех N-бензилиденанилиновых производных. Обсуждено влияние заместителей на конформации молекул на основании представлений о вращении ароматических колец.

STUDY OF THE SOLVENT EFFECT IN THE AMINE EXCHANGE OF
SCHIFF BASES, V.
CONNECTION BETWEEN THE RATE CONSTANT AND THE PARAMETERS
 E_T^N AND B_{KT} OF THE SOLVENT MIXTURES APPLIED

By

P. NAGY* and R. HERZFELD

Department of Chemistry, Gyula Juhász Teachers' Training
College, P.O.B. 396, H-6701 Szeged, Hungary

(Received 25th September, 1986)

The amine exchange of Schiff bases was studied in various solvent mixtures. With a regression equation, there was a good correlation between the rate constant and the solvent mixture parameters.

Introduction

We earlier studied the reactions of N-(2-hydroxybenzylidene)aniline and of N-(2-hydroxy-1-naphthylidene)aniline with n-butylamine and with benzylamine in ethanol-cyclohexane and in ethanol-benzene solvent mixtures [1-3]. The following correlation was found to hold between the rate constants and the activity coefficient of the ethanol in the solvent mixture [2, 3]:

$$\log k = x_1 \log k_1^* + x_2 \log k_2^* + (a_k + b_k \gamma_1) x_1 x_2 \quad (1)$$

where k , k_1^* and k_2^* are the rate constants in the mixture, in ethanol and in the aprotic solvent, respectively; x_1 and x_2 are the respective mole fractions; a_k and b_k are constants; and γ_1 is the activity coefficient of the ethanol in the mixture. Correlations similar to (1) hold for the acidity and basicity parameters measured in these solvent mixtures [4]:

$$E_T^N = x_1 (E_T^N)_1^* + x_2 (E_T^N)_2^* + (a_E + b_E \gamma_1) x_1 x_2 \quad (2)$$

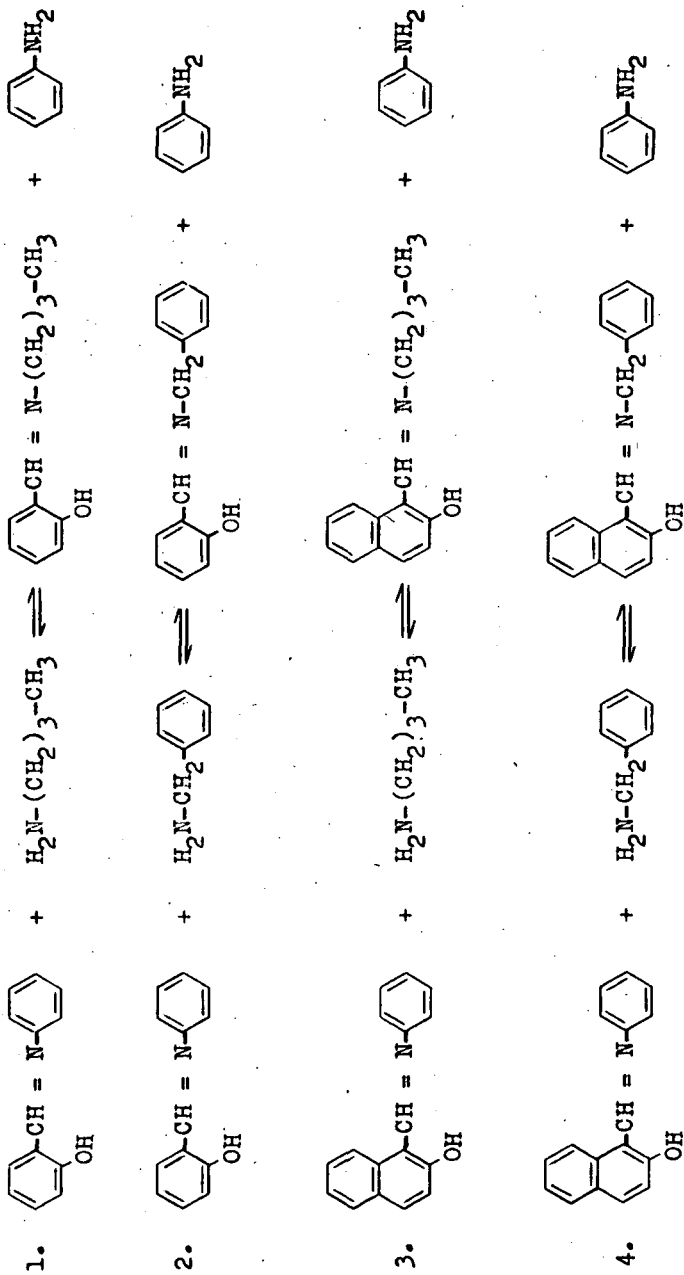
$$B_{KT} = x_1 (B_{KT})_1^* + x_2 (B_{KT})_2^* + (a_B + b_B \gamma_1) x_1 x_2 \quad (3)$$

The present paper reports on a study of the correlations between the acidity and basicity parameters and the rate of the amine exchange in ethanol-n-hexane, ethanol-cyclohexane and ethanol-benzene mixtures. The results provide further data promoting a better understanding of the mechanism of the amine exchange and of the solvent effect.

Experimental

The rate constants for reactions 1-4 were determined in ethanol-n-hexane, ethanol-cyclohexane and ethanol-benzene solvent mixtures with various compositions. Measurements were performed at 25°C. The reactions were followed spectrophotometrically.

The Dimroth-Reichardt $E_T(30)$ [5] and E_T^N [6] values were used to characterize the acidity of the solvent mixtures applied. The basicity was characterized with the Krygowski et al. [7] modification of the Kamlet-Taft [8] parameter B_{KT} [4]. The solvents were purified by means of the methods customary in spectroscopy, and were carefully freed from water.



Results and discussion

The rate constants for reactions 1-4 in ethanol-cyclohexane and in ethanol-benzene were reported earlier, as were the E_T^N and B_{KT} values for these mixtures [1, 2, 4]. The data relating to the ethanol-n-hexane mixtures are given in Table I.

Table I

E_T^N and B_{KT} data, and the log k values for reactions 1-4 in ethanol-n-hexane mixtures at 25°C

x_1	E_T^N	B_{KT}	log k			
			react.1	react.2	react.3	react.4
0.000	0.074*	0.00*	-	-	-	-
0.054	0.496	0.51	1.42	1.19	1.26	1.16
0.106	0.516	0.74	1.69	1.47	1.45	1.31
0.199	0.527	0.86	1.88	1.73	1.56	1.43
0.359	0.546	0.95	-	1.94	-	1.50
0.490	0.565	0.93	2.22	2.05	1.62	1.51
0.599	0.577	0.88	-	2.10	-	1.53
0.692	0.587	0.86	2.30	2.15	1.64	1.52
0.771	0.592	0.83	-	2.18	-	-
0.840	0.603	0.82	2.34	2.23	1.66	1.56
0.900	0.623	0.79	-	2.28	-	1.55
0.953	0.632	0.76	2.53	2.31	-	1.56
1.000	0.651	0.75	2.54	2.37	1.71	1.61

*Literature data [6, 7]

The literature contains a very large number of examples of correlations between the rate constants of various reactions and the solvent parameters. Correlations that are frequently used are

$$\log k = a + bE_T(30) \quad \text{and}$$

$$\log k = a + bE_T^N \quad (4)$$

For numerous reactions, these correlations adequately express the dependence of the rate constant on the acidity parameter of the solvent [9-12]. As pointed out by Reichardt, the $E_T(30)$ values of protolytic solvents (and hence the E_T^N values too) reflect the participation as donor in hydrogen-bonding, and thus the electrophilicity. Our earlier investigations demonstrated that the amine exchange of Schiff bases is influenced considerably by the ability of the solvent to form hydrogen-bonds. We therefore studied the correlation between the rate constants for reactions 1-4 in the various solvent mixtures and the corresponding E_T^N values in accordance with (4). The constants a and b calculated with the method of least squares are to be found in Table II.

Table II

Application of regression equation (4) to reactions 1-4 in various solvent mixtures

Reaction No.	Solvent mixture	a	b	n	r
1	ethanol-n-hexane	-1.905	7.027	8*	0.965
2		-2.072	7.067	12*	0.939
3		0.157	2.485	7*	0.875
4		0.155	2.300	11*	0.872
1	ethanol-cyclohexane	-2.209	7.728	13	0.990
2		-2.279	7.537	12	0.992
3		0.655	1.685	12*	0.918
4		0.480	1.806	12*	0.909
1	ethanol-benzene	-1.781	6.763	12	0.996
2		-2.157	7.000	12	0.999
3		-1.756	5.396	12	0.991
4		-2.092	5.774	12	0.994

*data ($\log k$, E_T^N) relating to the pure apolar solvent were not used in the calculations

The data in Table II reveal that the values of a and b are affected appreciably by the nature of the Schiff base. For example, the data for reactions 1 and 2 barely differ in the solvent mixtures employed (of similar type), but they differ considerably from the data for reactions 3 and 4. The correlation coefficients point to a relatively close correlation between $\log k$ and E_T^N . However, the $\log k$ values calculated in accordance with (4) with the a and b data in Table II frequently differ significantly from the measured data. This is illustrated in Figs 1 and 2.

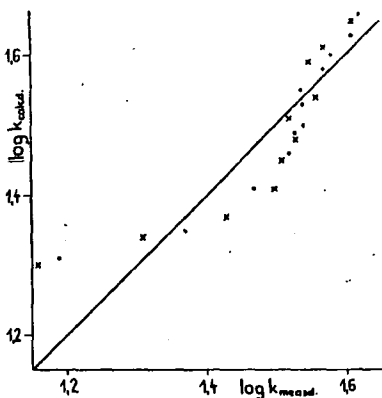


Fig. 1. Differences between the experimentally measured $\log k$ values for reaction 4 in ethanol-hexane (x) and ethanol-cyclohexane (.) mixtures and the values calculated via Eq. (4) with the data of Table II.

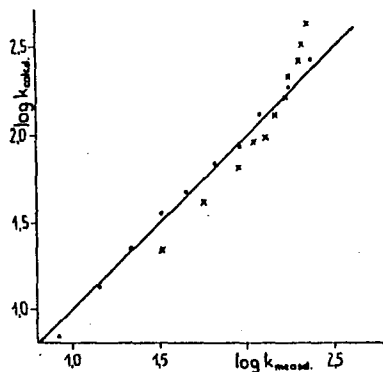


Fig. 2. Differences between the experimentally measured $\log k$ values for reaction 2 in ethanol-cyclohexane (x) and ethanol-benzene (.) mixtures and the values calculated via Eq. (4) with the data of Table II.

The differences between certain of the calculated and measured $\log k$ values are particularly large for reactions 3 and 4 in ethanol-n-hexane and in ethanol-cyclohexane mixtures. These differences, which are primarily to be observed in mixtures with low ethanol concentrations, indicate that it is not sufficient merely to take into account the acidity of the solvent for these systems; it is to be expected, for

instance, that the rate of the reaction is also influenced appreciably by the basicity of the solvent.

The use of a multiparameter equation to describe the solvent effect was introduced by Katritzky et al. [14]. In more recent investigations, a number of variations have been employed, in which use is made of the acidity and basicity parameters of the solvents, the molar refraction, the relative permittivity, the polarizability, the polarizing power, etc. A good review of the results to date is given by Svoboda et al. [15].

We have applied the following equation to describe the solvent effect observed in the amine exchange:

$$\log k = a + b_1 E_T^N + b_2 B_{KT} \quad (5)$$

where E_T^N and B_{KT} are the acidity and basicity parameters of the given solvent mixture, while a , b_1 and b_2 are constants characteristic of the system. A correlation of this type was effectively utilized by Krygowski and Fawcett [16-18] to characterize the solvent effect quantitatively in various processes. The experimental data [1, 2, 4] were employed with the method of least squares to determine the constants or (5) for reactions 1-4, and the corresponding multiple correlation coefficient (R) was calculated. In order to be able to compare the effects of the acidity and the basicity, we also converted the regression coefficients b_1 and b_2 to beta coefficients β_1 and β_2 , through the following equations [19, 17]:

$$\beta_1 = |b_1| \left(\frac{\sum_{i=1}^n (E_{T(d)}^N - \bar{E}_T^N)^2}{\sum_{i=1}^n (\log k_i - \overline{\log k})^2} \right)^{1/2}, \quad \beta_2 = |b_2| \left(\frac{\sum_{i=1}^n (B_{KT(d)} - \bar{B}_{KT})^2}{\sum_{i=1}^n (\log k_i - \overline{\log k})^2} \right)^{1/2} \quad (6)$$

where \underline{i} denotes the data measured in the given solvent, while $\overline{E_T^N}$, $\overline{B_{KT}}$ and $\overline{\log k}$ are average values for the \underline{n} experimental points. For the reactions in question, the distribution of the effects of the acidity and the basicity characteristic of the solvent was obtained as a percentage through the normalization of β_1 and β_2 [17]:

$$\beta_1' = \frac{100 \beta_1}{\beta_1 + \beta_2} \qquad \beta_2' = \frac{100 \beta_2}{\beta_1 + \beta_2} \qquad (7)$$

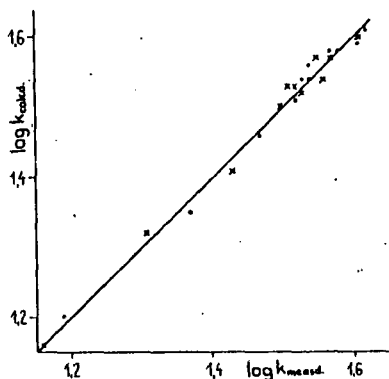


Fig. 3. Differences between the experimentally measured $\log k$ values for reaction 4 in ethanol-hexane (x) and ethanol-cyclohexane (•) mixtures and the values calculated via Eq. (5) with the data of Table III.

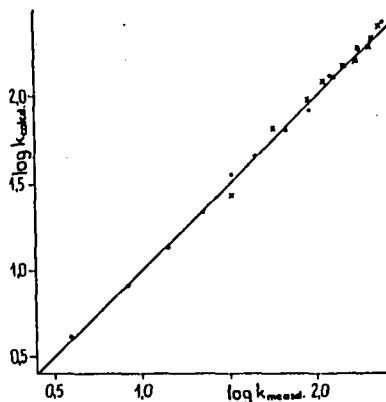


Fig. 4. Differences between the experimentally measured $\log k$ values for reaction 2 in ethanol-cyclohexane (x) and ethanol-benzene (•) mixtures and the values calculated via Eq. (5) with the data of Table III.

Figures 3 and 4 depict the measured $\log k$ values for some reactions, together with the calculated values obtained from the appropriate \underline{a} , \underline{b}_1 and \underline{b}_2 data in Table III.

Table III

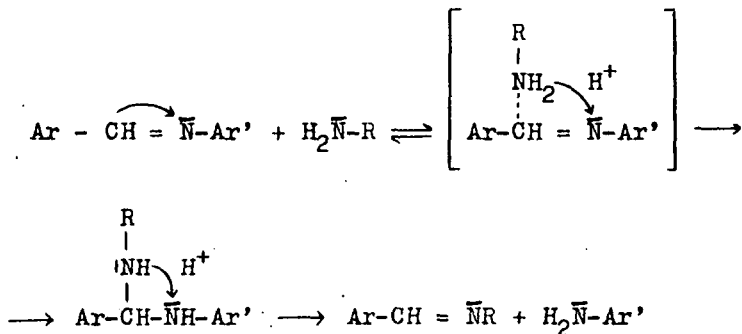
Application of regression equation (5) to reactions 1-4 in various solvent mixtures

Reaction No.	Solvent mixtures	a	b ₁	b ₂	β' ₁	β' ₂	n	R
1	ethanol-n-hexane	-2.196	6.371	0.855	76.70	23.30	8*	0.997
2		-2.614	6.515	1.065	71.90	28.10	12*	0.995
3		0.035	1.887	0.586	56.26	43.74	7*	0.994
4		-0.121	2.026	0.539	76.61	23.39	11*	0.995
1	ethanol-cyclohexane	-2.129	5.809	1.273	73.62	26.38	13	0.995
2		-2.227	5.186	1.598	67.20	32.80	12	0.999
3		0.501	1.284	0.477	61.58	38.42	12*	0.992
4		0.305	1.350	0.542	59.69	40.31	12*	0.993
1	ethanol-benzene	-1.978	8.201	-0.954	84.55	15.45	12	0.998
2		-2.300	8.037	-0.687	88.16	11.84	12	0.999
3		-2.065	7.645	-1.491	76.54	23.46	12	0.998
4		-2.347	7.628	-1.229	79.90	20.20	12	0.999

* data ($\log k$, E_T^N) relating to the pure apolar solvent were not used in the calculations

From a comparison of Figs 1-4 and Tables II and III, it may be stated that Eq. (5) gives a good description (essentially better than Eq. (4)) of the solvent effect observed in these reactions. The rate of amine exchange of the Schiff bases is therefore influenced by both the acidity and the basicity of the solvent applied.

This result confirms the previously assumed reaction mechanism [20], and makes it more exact. If the solvent effect too is taken into consideration, the main steps are expected to be as follows:



This mechanism is in accord with the experience that the amine exchange takes place with appreciable rate only in solvents capable of hydrogen-bonding both as donors and as acceptors. The hydrogen-bonds developing with the Schiff base and with the primary amine increase the electrophilic nature of the azomethine carbon atom, and also allow the proton transfers to occur through mediation of the solvent. Clearly, both effects increase the reaction rate.

The data in Table III reveal that, in all three solvent mixtures, the effect of the acidity is more significant than that of the basicity. It is also noteworthy that both b_1 and b_2 are positive in the ethanol-hexane and ethanol-cyclohexane mixtures, whereas in the ethanol-benzene mixtures b_2 is negative. In our opinion, this does not mean

that the basicity increases the reaction rate in the ethanol-cyclohexane mixtures, for instance; and decreases it in the ethanol-benzene mixtures. The negative sign may arise as a computational result in consequence of the interaction between the ethanol and benzene molecules, or of the composition-dependent changes in the mixture. This fits in with our earlier finding that the E_T^N values, and particularly the B_{KT} values, vary in appreciably different ways as functions of the mixture composition in ethanol-cyclohexane and ethanol-benzene mixtures [4].

References

- [1] Nagy, P.: Juhász Gy. Tanárképző Főisk. Tud. Közl. 114 (1982)
 - [2] Nagy, P.: Acta Chim. Hung. 112, 461 (1983)
 - [3] Gulyás, I., Nagy, P.: Magy. Kém. Lapja, 39, 234 (1984)
 - [4] Nagy, P., R. Herzfeld: Acta Phys. et Chem. Szeged, 31, 735 (1985)
 - [5] Dimroth, K., C. Reichardt, T. Siepmann, F. Bohlmann: Liebigs. Ann. Chem. 661, 1 (1963)
 - [6] Reichardt, C., E. Harbusch-Görnert: Liebigs. Ann. Chem. 721 (1983)
 - [7] Krygowski, T.M., E. Milczarek, P.K. Wrona: J.C.S. Perkin II. 1563 (1980)
 - [8] Kamlet, M.J., R.W. Taft: J. Amer. Chem. Soc. 98, 377 (1977)
 - [9] Elias, H., G. Gumbel, S. Neitzel, H. Volz: Fresenius Z. Anal. Chem. 306, 240 (1981)
 - [10] Elias, H., K.J. Wannowius: Inorg. Chem. Acta 64, L 157 (1982)
 - [11] Reichardt, C.: Pure Appl. Chem. 54, 1867 (1982)
 - [12] Reichardt, C.: Molecular Interactions, Wiley, Chichester, New York, Vol. 3, p. 241 (1982)
 - [13] Reichardt, C.: Angew. Chem. 91, 119 (1979)
 - [14] Fowler, F.W., A.R. Katritzky, R.J.D. Rutherford: J. Chem. Soc. B 460 (1971)
 - [15] Svoboda, P., O. Pytela, M. Vecera: Collection Czechoslovak Chem. Commun. 48, 3287 (1983)
 - [16] Krygowski, T.M., W.R. Fawcett: Aust. J. Chem. 28, 2115 (1975)
 - [17] Krygowski, T.M., W.R. Fawcett: J. Amer. Chem. Soc. 97, 2143 (1975)
 - [18] Krygowski, T.M., W.R. Fawcett: Can. J. Chem. 54, 2383 (1976)
 - [19] Ezekiel, M., K.A. Fox: "Methods of correlation and Regression Analysis" 3rd ed, Wiley, New York, 1959.
 - [20] Cordes, E.H., W.P. Jencks: J. Amer. Chem. Soc. 84, 826 (1962)
- Nagy, P.: Magy. Kém. Folyóirat, 78, 158 (1972)

ИССЛЕДОВАНИЕ ВЛИЯНИЯ РАСТВОРИТЕЛЯ ПРИ
АМИНООБМЕНЕ ОСНОВАНИЙ ШИФФА, V.

Связь коэффициента скорости с параметрами E_T^N и V_{KT}
применяемых растворителей

П. Надь и Р. Херцфельд

Нами был исследован аминокобмен оснований Шиффа в различных растворителях. По одному регрессивному уравнению установлена хорошая корреляция между коэффициентом скорости и параметрами E_T^N и V_{KT} растворителей.

LIQUID-PHASE RADICAL REACTIONS OF ACETALS AND
THEIR ANALOGUES AT HIGH PRESSURE

by

V. M. Zhulin,¹ V. V. Zorin,² S. S. Zlotskii,²
D. L. Rakhmankulov,² M. Bartók³ and Á. Molnár³

¹N. D. Zelinsky Organic Chemistry Institute,
USSR Academy of Science, USSR

²Ufa Oil Institute, Ufa, USSR

³Department of Organic Chemistry, József Attila
University, Szeged, Hungary

(Received 25th November, 1986)

Results, concerning the influence of high pressure on the rates and directions of homolytic transformations of cyclic, linear-cyclic and linear acetals and their N- and S-containing heteroanalogues are summarized and analyzed.

High pressure is widely used to obtain information on the mechanism of chemical reactions, the structures of the transition states, and the effects of various factors on the rates and directions, i.e. it is used for purposes of chemical synthesis [1-4]. Just as data can be obtained on the energy parameters in the knowledge of the displacement of equilibrium and the variations in the process rates with changes in temperature, the volume characteristics of reactions behave as thermodynamic variables with the variation of pressure.

It has been established on the basis of transition state theory that the rate of reaction depends on pressure (p) (Eq. (1)), where ΔV^\ddagger is the volumetric activation effect, numerically equal to the

$$\left(\frac{\partial \ln k}{\partial p} \right)_T = \frac{\Delta V^\ddagger}{RT} \quad (1)$$

change in volume on the formation of one mole of the activ-

ated complex from the interacting particles.

An analogous equation is known from chemical thermodynamics. It characterizes the dependence of the equilibrium constant on pressure, but instead of ΔV^\ddagger it contains ΔV , the volumetric change during the reaction. Equation (1) shows that k decreases with the increase of pressure, if $\Delta V^\ddagger > 0$, i.e. if, during the formation of the transition state from the initial particles, a volume increase occurs. For example, it may be presumed that in the homolytic decay of tert-butyl peroxide the breaking bond O-O is lengthened in the transition state and the volume of the latter will be larger than that of the initial molecule. Indeed, the known data show that the decay rate of tert-butyl peroxide decreases with the increase of pressure.

The majority of chemical reactions are accelerated by the increase of pressure ($\Delta V^\ddagger < 0$) as they are bimolecular. In the formation of the transition state in a bimolecular reaction, the initial particles come so close together that the distance between them is less than the sum of their van der Waals radii. As a result, the volume of the transition state is less than the sum of the volumes of the initial particles. Radical addition reactions to a double bond (the growth of the chain during polymerization), for instance, and the extraction of H and Cl atoms by a radical (radical substitution) accelerate with pressure increase.

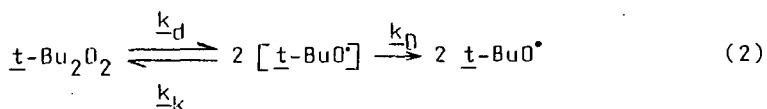
Among free radical reactions there are fast processes (such as recombination and disproportionation), including the termination step in radical-chain processes, the rate of which is determined by diffusion factors and therefore depends on the viscosity of the medium. Since the viscosity increases considerably with the increase of pressure, the rates of such reactions decrease, though they remain bimolecular. On the other hand, it is not difficult to imagine that monomolecular radical reactions might also be accelerated by pressure, e.g. the formation of cyclic radicals from linear radicals by intramolecular addition of a free radical centre to an unsaturated bond. This may be expected because the density of cyclic combinations is usually higher

than that of the linear combinations containing the same number of atoms in the chain.

The value of ΔV^\ddagger is determined experimentally by measuring the rates of reaction at different pressures. The logarithm of the rate constant is then plotted against pressure. ΔV^\ddagger is calculated by analytical or graphical differentiation of this function in accordance with Eq. (1) at the point of atmospheric pressure. As the function is usually non-linear, the differentiation method requires a large number of exact experimental data, and even then some uncertainties remain. In this respect, a number of methods for the calculation of ΔV^\ddagger have been suggested. Among them, a very simple method deserves attention. This was proposed by Gonikberg and El'yanov [1, 5] and is based on the linear correlation of free energies with the change of pressure. This method allows the determination of ΔV^\ddagger from a limited number of data, through the linear dependence of $\log k$ on Φ , characterizing the pressure. This method is used in the present work.

The kinetically determined rate of reaction is usually a complex constant, including several rate constants of more or less simple reactions, connected with each other in different ways depending on the process mechanism. In such cases the volumetric activation effect ΔV^\ddagger is obtained from the function $\log k$ vs. p . The essence of the volumetric activation effect can be seen in the following example.

tert-Butyl peroxide ($t\text{-Bu}_2\text{O}_2$) decay may be represented schematically as in Eq. (2), where the



square brackets designate a cage of solvent molecules. Radicals in the cell may either diffuse from the cell with rate constant k_f , or recombine inside the cell (k_k) with formation of the initial peroxide (k_d is the rate of radical formation in the cell).

The rate of decay w_p may be presented as in Eq (3), where f is the fraction of radicals leaving

$$\underline{w}_p = 2 f k_d [C] \quad (3)$$

the cell, connected with the rate constants k_k and k_D by the dependence $\frac{1-f}{f} = \frac{k_k}{k_D}$, and $[C]$ is the concentration of peroxide. Therefore, $\frac{k_D}{k_p} = 2f k_d$. Taking logarithms, with subsequent differentiation with respect to p and multiplication by RT gives Eqs. (4) and (5).

$$\Delta \underline{V}_p^\ddagger = \Delta \underline{V}_d^\ddagger + \Delta \underline{V}_f^\ddagger \quad (4)$$

$$\Delta \underline{V}_f^\ddagger = -RT \left(\frac{\partial \ln f}{\partial p} \right)_T \quad (5)$$

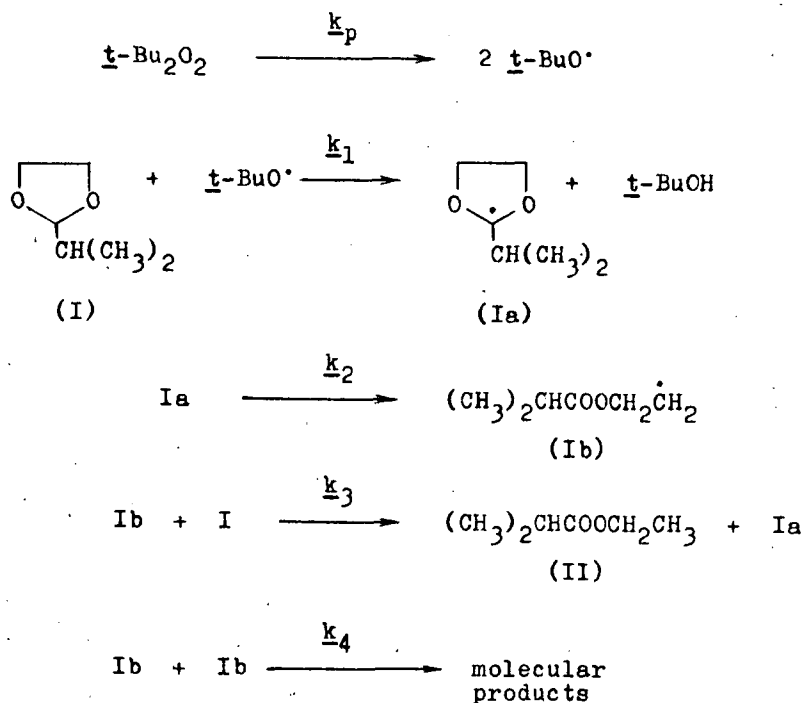
The present article considers generalized information on the influence of high pressure on the rates and directions of the homolytic transformation of acetals in solution.

It is known that linear and cyclic acetals [6-9] and their nitrogen- and sulphur-containing analogues [10-13] are transformed in the presence of radical initiators at 393-423 K into carboxylic esters, amides or thioesters, respectively.

The process has a non-ramified chain free radical mechanism with a quadratic termination on rearranged (eliminated in the case of linear acetals) radicals [6,7, 10].

The limiting stage of isomerization (fragmentation) is the reaction of hydrogen atom abstraction from the substrate by a rearranged radical [6, 7, 10]. These reactions are characterized by very short chain length, and therefore by a high specific expenditure of initiator. Attempts have been made by some authors to intensify these reactions through the application of high pressure and to study its influence on the kinetics and mechanisms of these reactions.

Thus, in the homolytic liquid-phase isomerization of 2-isopropyl-1,3-dioxolane (I) into ethyl isobutyrate (II) (Scheme I), initiated by $t\text{-Bu}_2\text{O}_2$ at 403 K and pressure up to 10000 kg/cm² [14, 15] the decay rate constant of $t\text{-Bu}_2\text{O}_2$, k_p , decreases. The length of the kinetic chain ($\bar{\nu}$), defined as the ratio of the initial rate of ethyl isobutyrate formation (\underline{w}_{II}) to the rate of initiation (\underline{w}_i), numerically equal to the accumulation rate of tert-butyl



Scheme I

alcohol ($w_i = w_{\text{t-BuOH}}$), increases a little with the increase of pressure.

A considerable decrease of the initiation rate, which is not compensated by a small increase of the kinetic chain length at the same time, is the cause of the formation rate decrease of ester II at increasing pressure. The kinetic parameter $k_3/\sqrt{k_4}$, characterizing the reactivity of 2-isopropyl-1,3-dioxolane (I) in free radical isomerization, practically does not change with the change of pressure (Table I), which means that $\Delta V_3^\ddagger - \frac{1}{2} \Delta V_4^\ddagger \approx 0$.

In the discussed process, the chain is propagated by carbon-centred radicals; in the abstraction of hydrogens, ΔV^\ddagger is negative but has a comparatively small value: $\Delta V_3^\ddagger \approx -4 \text{ cm}^3/\text{mol}$ [14, 15, 18]. At $\Delta V_3^\ddagger - \frac{1}{2} \Delta V_4^\ddagger \approx 0$; $\Delta V_4^\ddagger \approx 8 \text{ cm}^3/\text{mol}$, i.e. the termination is accelerated by pressure and proceeds

not in the diffusion but in the kinetic sphere [3]. The conclusion of the acceleration of the termination with pressure increase is true only when the cyclic radical does not play a perceptible part in the termination.

Thus, the increase of pressure does not lead in this case to acceleration of the process, but decreases the expenditure of the initiator approximately 3-fold, at the expense of the increase in length or the kinetic chain from 5 to 14 (Table I).

Isomerization of non-symmetric cyclic acetals leads to the formation of two isomeric esters [16]. Thus, the reaction of 4-methyl-1,3-dioxane (III) initiated by $t\text{-Bu}_2\text{O}_2$ at 403 K yields *n*-butyl formate (IV) and *sec*-butyl formate (V) in a ratio of 6:1 at normal pressure [16] (Scheme II). In refs. [15, 17], the influence of high pressure on the products of this reaction was studied; for this purpose the kinetics of accumulation of esters IV and V at various pressures was investigated.

With the increase of pressure, as with 2-isopropyl-1,3-dioxolane, the initiation rate in the system decreases similarly to the rate constant of $t\text{-Bu}_2\text{O}_2$ decay (k_p) [15, 17] (Table II). With the increase of pressure, the selectivity of formation of *n*-butyl formate (IV) increases. This can be explained in that in the process of monomolecular rearrangement of the 4-methyl-1,3-dioxo-2-cyclohexyl radical (IIIa) in the transition state the C(4)-O(3) bond is lengthened to a smaller extent than the C(6)-O(1) bond, the result being that the volume increase is greater in activation in the latter case. The difference in the volumetric activation effects of the C(6)-O(1) and C(4)-O(3) bonds is $3.0 \text{ cm}^3/\text{mol}$.

Parameter $k_3/\sqrt{k_4}$, characterizing the reactivity of 4-methyl-1,3-dioxane (III) in the free radical isomerization, increases a little, while the kinetic chain length \bar{v} increases more with pressure (up to 7500 kg/cm^2) than in the case of 2-isopropyl-1,3-dioxolane (I). This is possibly connected with the fact that in 4-methyl-1,3-dioxane isomerization secondary formyloxybutyl radicals (IVa) take part in the chain lengthening and the reaction accelerates more

Table I

Liquid-phase radical isomerization of 2-isopropyl-1,3-dioxolane (I) to ethyl isobutyrate (II) under high pressure [14, 15]

$T = 403 \text{ K}$, $\tau = 2 \text{ hr}$, $[t\text{-Bu}_2\text{O}_2] = 0.4 \text{ mol/l}$, $[I] = 7.6 \text{ mol/l}$

Pressure (kg/cm ²)	[II] (mol/l)	[t-BuOH] (mol/l)	$w_{II} \cdot 10^5$ (mol/l.s)	$w_{t\text{-BuOH}} \cdot 10^5$ (mol/l.s)	ν	$k_p \cdot 10^5$ (s ⁻¹)	$\frac{k_3^a}{\sqrt{k_4}} \cdot 10^3$
1	0.55	0.11	7.6	1.5	5.0	1.9	3.6
2000	0.56	0.06	7.8	0.9	9.0	1.1	4.9
5000	0.38	0.03	5.3	0.4	12.2	0.5	4.7
10000	0.22	0.02	3.1	0.2	14.2	0.27	3.9

$$\frac{k_3^a}{\sqrt{k_4}} = \frac{w_{II}}{[I] \sqrt{w_{t\text{-BuOH}}/2}}$$

Table II

Dependence of formation rate of n-butyl formate (IV) and sec-butyl formate (V) and constants k_p and $k_3/\sqrt{k_4}$ on pressure in 4-methyl-1,3-dioxane (III) isomerization [15]. $T = 403$ K, $[t\text{-Bu}_2\text{O}_2] = 0.5$ mol/l, $[\text{III}] = 7.0$ mol/l

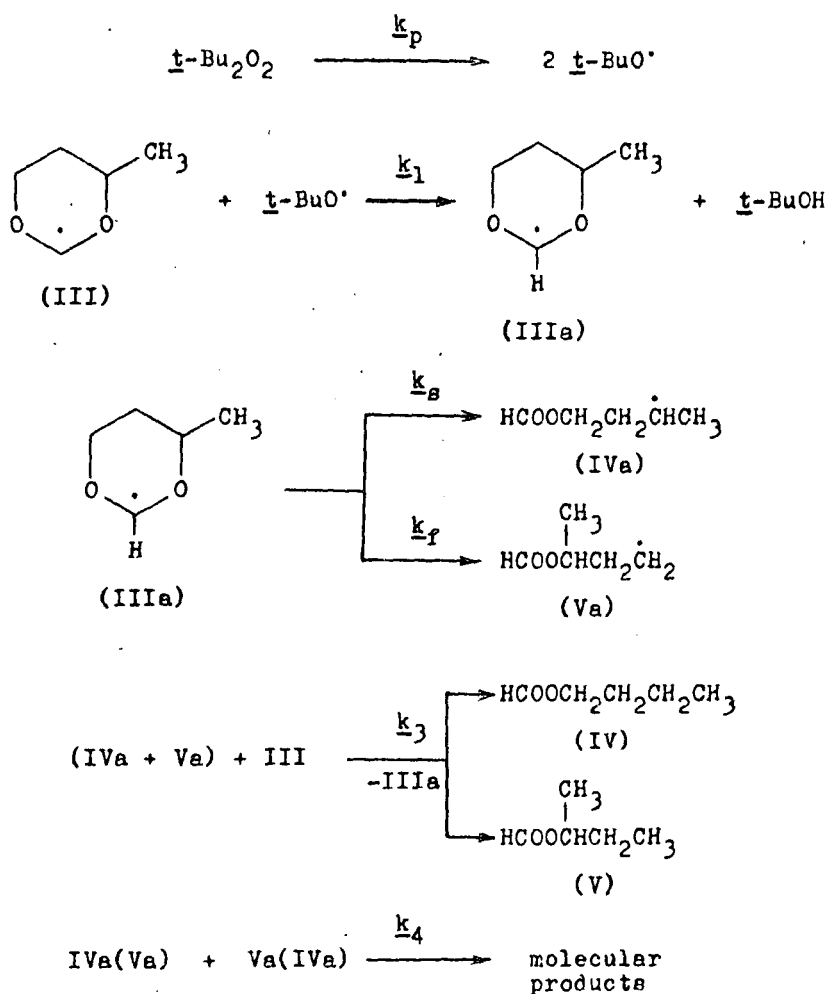
Pressure (kg/cm ²)	$w_{t\text{-BuOH}}$ (mol/l.s)	$k_p \cdot 10^6$ (s ⁻¹)	$w_{IV} \cdot 10^5$ (mol/l.s)	$w_V \cdot 10^5$ (mol/l.s)	$\frac{w_{IV}}{w_V}$	w_{IV+V}^a (mol/l.s)	v^b	$\frac{k_3}{\sqrt{k_4}} \cdot 10^3$ (l/mol.s) ^{1/2}
1	2.7	27.0	1.85	0.31	5.9	2.2	0.8	0.9
2500	1.6	16.0	2.40	0.33	7.2	2.7	1.7	1.4
5000	1.2	12.0	2.55	0.32	8.0	2.9	2.4	1.6
7500	0.6	5.8	2.1	0.25	8.6	2.4	3.9	2.2
10000	0.3	2.9	0.05	0.08	10.0	0.9	3.1	1.1

$$^a w_{IV+V} = w_{IV} + w_V$$

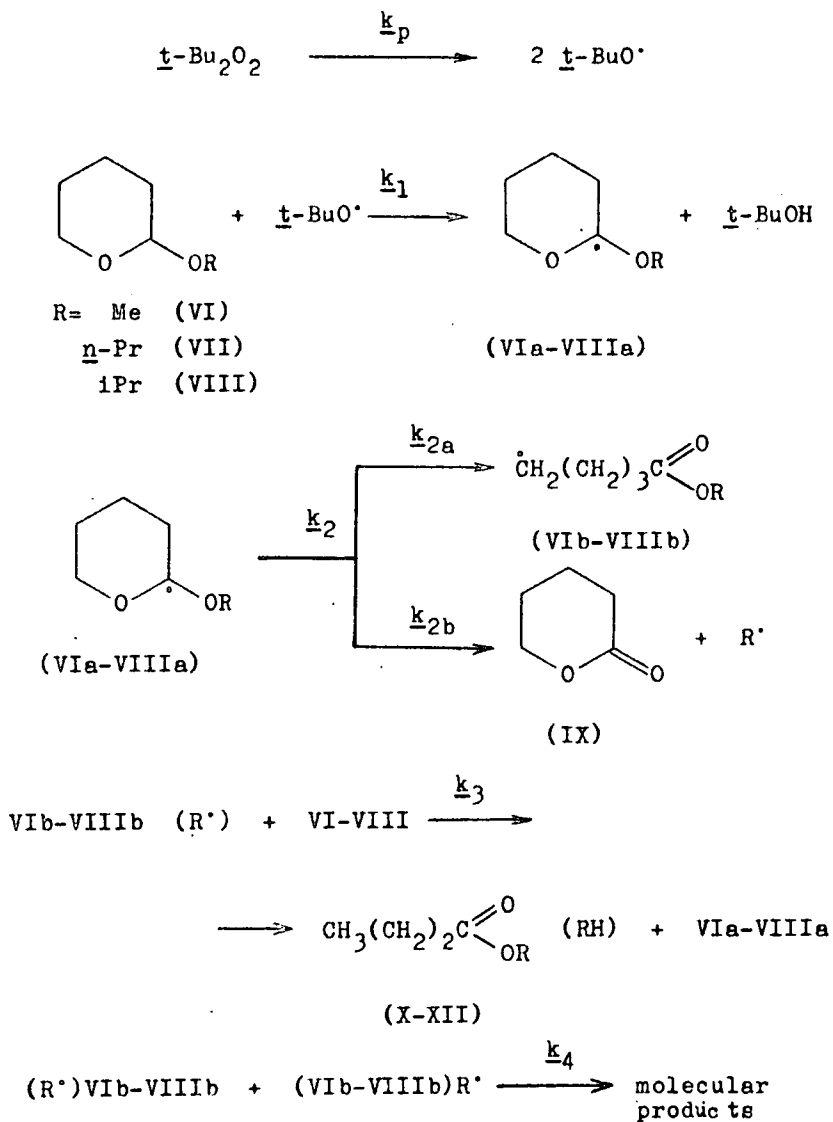
$$^b v = w_{IV+V} / w_{t\text{-BuOH}}$$

quickly in their presence [18].

It has already been shown [19, 20] that the homolytic transformation of linear-cyclic acetals of 2-alkoxytetrahydropyrans (VI-VIII), initiated by $t\text{-Bu}_2\text{O}_2$ at 403 K, leads to the formation of two products: δ -valerolactone (IX) and the corresponding alkyl ester of valeric acid (X-XII) (Scheme III). As a result of experiments with compounds



Scheme II



Scheme III

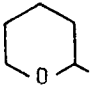
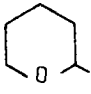
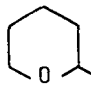
VI-VIII at different pressures, it has been established that the reaction products do not change qualitatively, but the correlation of the isomerization products (k_{2a}) and fragmentation products (k_{2b}) depends essentially on pressure [21, 22].

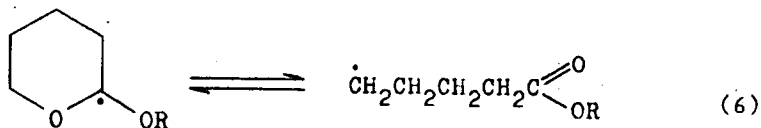
With pressure increase, the ratio of lactone to ester is increased (Table III). Thus, at atmospheric pressure 2-methoxytetrahydropyran (VI) is transformed almost entirely into the isomeric ester methyl valerate (X), while at 10000 kg/cm^2 the yield of δ -valerolactone (IX) is close to that of ester X. The observed change in the lactone:ester ratio (scores of times for VI) in response to pressure is impossible to explain [21, 22] by the difference in chain lengthening alone on the formation of the transition state. From the difference in volumetric activation effect of the two reactions (lactone formation and ester formation from VI) the quantity of $25 \text{ cm}^3/\text{mol}$ is obtained, which is incompatible with any chain lengthening in the cycle. The most probable explanation of the observed effect is an equilibrium (Eq. (6)). With the increase of pressure, this equilibrium is shifted to the left for the formation of a compound with higher density, the volumetric effect of this reaction being nearly $15 \text{ cm}^3/\text{mol}$. This suggestion provides at least a qualitative explanation of the results obtained. In the presence of the equilibrium, the lactone:ester ratio is connected with a large number of kinetic parameters and numerical interpretation of the results is in general very difficult problem. The above feature allows an explanation of the comparatively small change in the lactone:ester ratio (less than 3-fold at 10000 kg/cm^2) for VIII. It is quite possible that in this case cyclization does not take place, for example, because of spatial difficulties and because of the presence of the bulkier isopropyl group, the lactone:ester ratio being determined by the fission rate ratio of the corresponding bonds. In such cases the change in the lactone:ester ratio under pressure will be determined by the difference in the transition state volumes, originating from the lengthening of the endo- and exocyclic bonds. According to Table III this difference averages $6 \text{ cm}^3/\text{mol}$,

Table III

Homolytic transformations of 2-alkoxytetrahydropyrane at high pressure [21, 22]

 $T = 403 \text{ K}$, $[t\text{-Bu}_2\text{O}_2] = 0.3 \text{ mol/l}$, $\tau = 2 \text{ hr}$

Compound (mol/l)	Pressure (kg/cm ²)	[lactone].10 (mol/l)	[ester].10 (mol/l)	$\frac{[\text{lactone}]}{[\text{ester}]}$	[t-BuOH].10 (mol/l)	ν_{ester}	ν_{Σ}
 VI (8.26)	1	0.05	3.50	0.01	1.20	2.9	2.96(3.0)
	2500	0.15	2.00	0.07	0.45	4.4	4.77(4.8)
	5000	0.35	1.50	0.23	0.20	7.5	9.2
	7500	0.45	0.90	0.50	0.10	9.0	13.5
 VII (6.42)	10000	0.50	0.70	0.70	0.10	7.0	12.0
	1	0.29	1.43	0.20	0.78	1.8	2.2
	2500	0.25	0.75	0.33	0.28	2.7	3.6
	5000	0.23	0.30	0.77	0.20	1.5	2.6
 VIII (6.47)	10000	0.18	0.10	1.80	0.12	0.8	2.3
	1	0.80	0.25	3.20	0.77	0.3	1.4
	2500	0.70	0.20	3.50	0.28	0.7	3.2
	5000	0.55	0.10	5.50	0.16	0.6	4.1
	10000	0.45	0.05	9.00	0.08	0.6	6.2



which seems quite admissible.

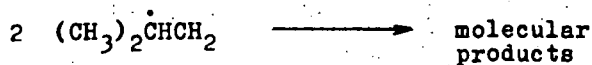
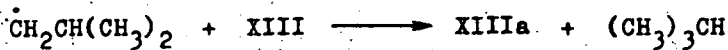
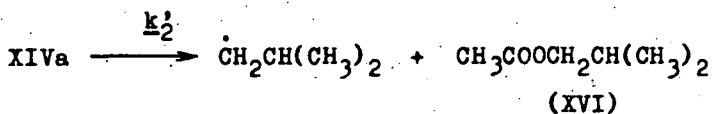
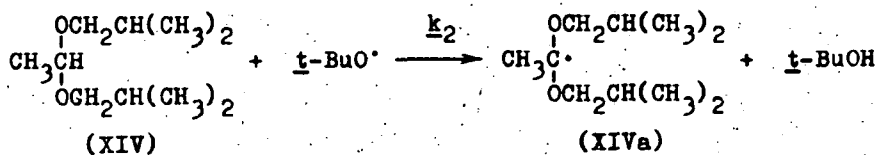
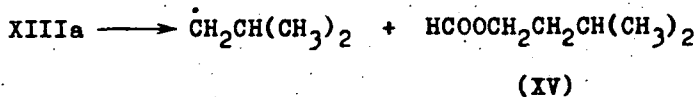
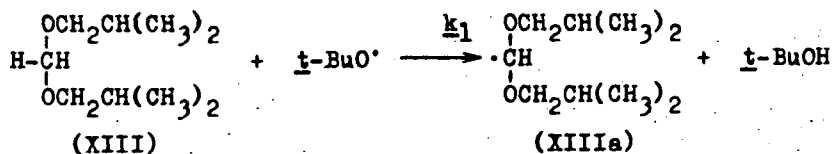
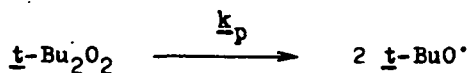
Homolytic transformations of linear acetals under high pressure has been investigated on the examples of diisobutoxymethane (XIII) and 1,1-diisobutoxyethane (XIV), which were converted into isobutyl formate (XV) and isobutyl acetate (XVI) in reactions initiated by $t\text{-Bu}_2\text{O}_2$ at 403 K [23, 24].

The transformations of acetals XIII and XIV under the influence of $t\text{-Bu}_2\text{O}_2$ (in accordance with [7-9]) are described by Scheme IV in which the termination is the result of recombination in the presence of radicals $\text{CH}_2\text{CH}(\text{CH}_3)_2$.

The simultaneous formation of esters XV and XVI is a result of a chain process in which two substrates are involved. The formation rate ratio of the esters, $\frac{w_{\text{XV}}}{w_{\text{XVI}}}$, is determined by the difference in the reactivities of acetals XIII and XIV, i.e. by the tendencies of the corresponding C(1)-H bonds, adjacent to the two oxygen atoms, to undergo homolytic breaking [23, 24]. With the increase of pressure the initiation rate in the system decreases, which in turn causes a decrease in the rates of formation of esters XV and XVI (Table IV).

The difference in the activities of acetals XIII and XIV increases under pressure (Table IV), as demonstrated by the ratio of the formation rates of isobutyl acetate and isobutyl formate, $\frac{w_{\text{XVI}}}{w_{\text{XV}}}$, i.e. under pressure the homolytic breaking of the tertiary bond C(1)-H in 1,1-diisobutoxyethane increases to a greater degree under the influence of the radical $\text{CH}_2\text{CH}(\text{CH}_3)_2$ [23, 24]. A similar regularity has been found for substitution reactions in the presence of oxygen-centred radicals [25].

During the thermal decay of $t\text{-Bu}_2\text{O}_2$ at 403 K in a medium of N-propyl-1,3-oxazolidine (XVII) or N-propyl-2-ethyloxazolidine (XVIII), N-ethyl-N-propylformamide (XIX)



Scheme IV

Table IV

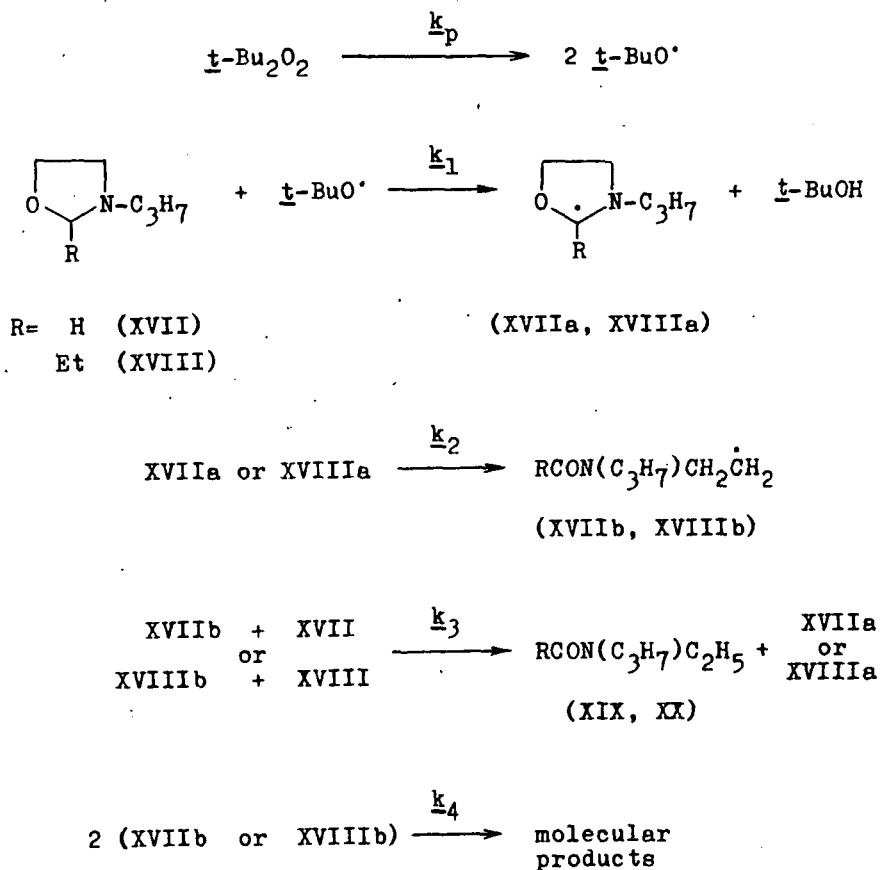
Homolytic transformations of 1,1-diisobutoxyalkanes (XIII, XIV) in the liquid phase at high pressure [23, 24]

$T = 403 \text{ K}, [t\text{-Bu}_2\text{O}_2] = 0.4 \text{ mol/l}, [\text{XIII}] = [\text{XIV}] = 2 \text{ mol/l}$

Pressure (kg/cm ²)	$\frac{w_{t\text{-BuOH}}}{\text{mol/l.s}} \cdot 10^6$	$k_p \cdot 10^6$ (s ⁻¹)	$\frac{w_{\text{XV}}}{\text{mol/l.s}} \cdot 10^6$	$\frac{w_{\text{XVI}}}{\text{mol/l.s}} \cdot 10^6$	$\frac{w_{\text{XVI}}^a}{w_{\text{XV}}}$	ν
100 - 200	50.0	62.5	63.0	44.0	1.4	2.1
2500	37.3	46.5	37.5	23.0	1.7	1.6
5000	24.0	30.0	35.5	18.1	2.0	2.2
7500	13.9	17.4	32.0	13.8	2.4	3.8
10000	9.6	12.0	21.8	7.0	3.1	3.0

$$\frac{w_{\text{XVI}}^a}{w_{\text{XV}}} = \frac{k_3'}{k_3}$$

or *N*-ethyl-*N*-propylpropionamide (XX) is formed [26, 27]. At high pressure (1-10000 kg/cm²), the composition of the products does not change qualitatively [26, 27]. The formation of amides XIX and XX follows Scheme V [10]. With the increase of pressure from 1 up to 10000 kg/cm², both the initiation rate ($\underline{w}_i = \underline{w}_{t\text{-BuOH}}$) and the decay rate constant of $t\text{-Bu}_2\text{O}_2$ decrease by one order (Table V). The formation rates

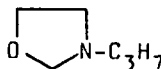
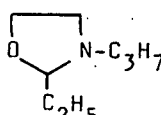


Scheme V

Table V

Kinetic parameters of homolytic liquid-phase isomerization of 1,3-oxazolidines (XVII, XVIII) under high pressure [26, 27]

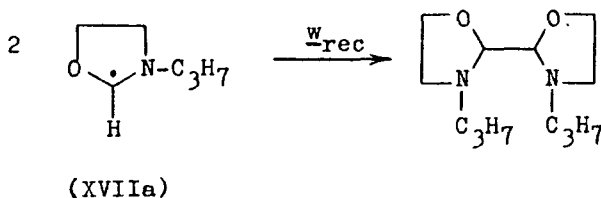
$T = 403 \text{ K}$, $[t\text{-Bu}_2\text{O}_2] = 0.4 \text{ mol/l}$ $\tau = 2 \text{ hr}$, solvent = chlorobenzene

1,3-oxazolidines	Pressure (kg/cm ²)	[t-BuOH] (mol/l)	$\frac{w_{t\text{-BuOH}}}{10^5}$	$\frac{k_p}{s^{-1}} \cdot 10^5$	[amide] (mol/l)	$\frac{w_{\text{amide}}}{10^5}$	v^a
	1	0.25	3.5	4.3	0.32	4.4	1.3
	2500	0.12	1.7	2.1	0.03	0.3	0.2
	5000	0.09	1.3	1.6	0.02	0.3	0.2
	7500	0.07	1.0	1.2	0.01	0.1	0.1
	10000	0.04	0.5	0.5	-	-	-
	1	0.25	3.5	4.4	0.38	5.4	1.5
	2500	0.10	1.4	1.8	0.06	0.9	0.6
	5000	0.08	1.1	1.4	0.01	0.2	0.1
	7500	0.06	0.9	1.2	0.01	-	-
	10000	0.03	0.3	0.4	-	-	-

$$a \quad v = \frac{w_{\text{amide}}}{w_{t\text{-BuOH}}}$$

of amides XIX and XX at the same pressure decrease together with the length of the kinetic chain, in contrast with the transformations of cyclic [14], linear-cyclic [21] and linear [23] acetals.

Consideration of all the data testifies to the fact that, in the oxazolidine reactions, chain opening takes place in the cyclic radicals too. This has been confirmed in work [28] in which the ratio of the rates of formation and recombination of cyclic radicals XVIIa (w_{rec}) and of initiation (w_i) at 1 and 7500 kg/cm² was determined (Scheme VI).



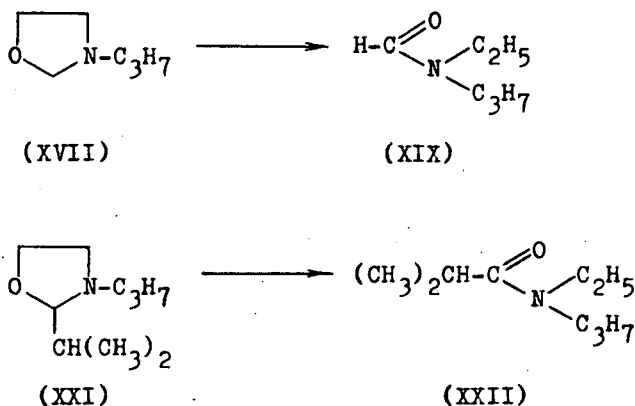
Scheme VI

At a pressure of 1 kg/cm² the ratio $2 w_{rec}/w_i = 0.1$, i.e., only 10% of the cyclic radicals formed take part in recombination while at a pressure of 7500 kg/cm² the ratio $2w_{rec}/w_i = 0.4$, i.e. the number of cyclic radicals XVIIa taking part in the recombination increases 4-fold. Thus, with the increase of pressure rate of monomolecular rearrangement of 1,3-oxaza-2-cyclopentyl radical into linear radical XVIIb decreases sharply, while the proportion of cyclic radicals XVIIa taking part in chain opening increases.

The most probable explanation is that pressure accelerates the recombination of cyclic radicals (termination) and slows down the rate of their rearrangement into linear radicals. Further, the latter effect is possibly essential as is the case with the existence of the cyclic radical \rightleftharpoons linear radical equilibrium in the tetrahydropyran reactions (Eq. (6)). This increase in the number of radicals taking part in the termination corresponds to a

volumetric activation effect of $14 \text{ cm}^3/\text{mol}$, which is difficult to explain by the difference in chain lengthening alone.

Thus, in [26, 27] the influence of high pressure on the relative activity of 1,3-oxazolidines (XVII, XXI) (Scheme VII) in radical isomerization was studied via the



Scheme VII

competing reactions method and it was established that with the increase of pressure up to 2500 g/cm^2 the relative yield of the N-ethyl-N-propylisobutyramide (XXII), which is isomeric to 2-isopropyl-N-propyl-1,3-oxazolidine (XXI), increases in comparison with that of the formamide XIX formed from N-propyl-1,3-oxazolidine (XVII) (Table VI). This increase conforms to a volumetric activation effect of $14 \text{ cm}^3/\text{mol}$, the difference in chain lengthening hardly being the reason for this.

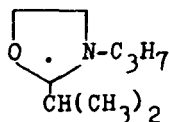
The most logical explanation seems to be that in one of the cases (compound XXI) the linear rearranged radical does not recycle, while the other case (compound XVII) is characterized by the equilibrium cyclic radical \rightleftharpoons linear radical being displaced, as noted above, to the left. Such a difference in the volumetric effects as $14 \text{ cm}^3/\text{mol}$ is then possible. Unfortunately, this is not the only "logical" explanation. As pointed out above, a recombination reaction

Table VI

Influence of high pressure on the relative activity of 1,3-oxazolidines in radical isomerization [26, 27].
 $T = 403 \text{ K}$, $[t\text{-Bu}_2\text{O}_2] = 0.5 \text{ mol/l}$, $[\text{XVII}] = [\text{XXI}] = 2 \text{ mol/l}$,
 solvent = chlorobenzene

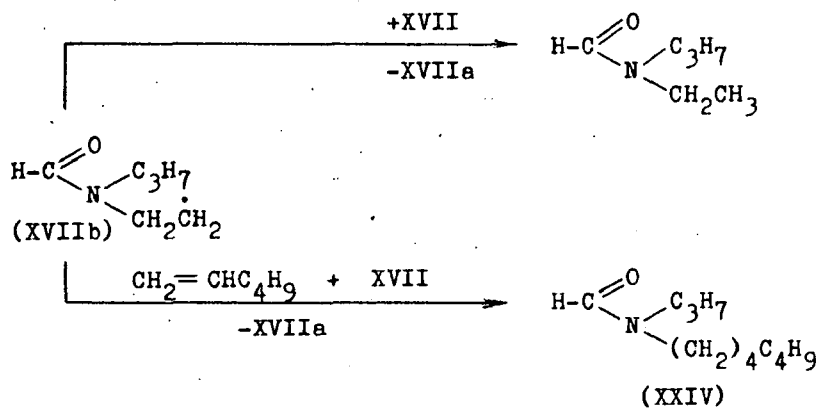
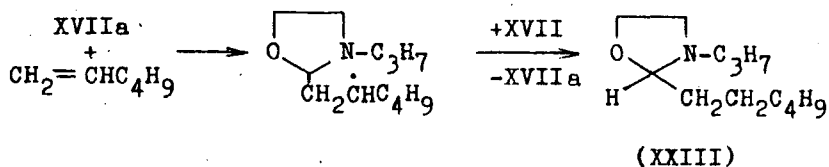
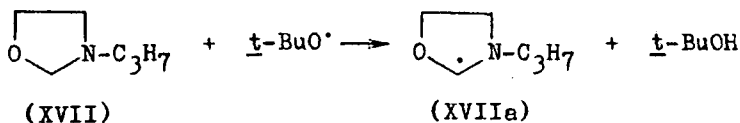
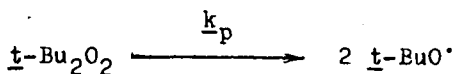
Pressure (kg/cm ²)	[XIX] (mol/l.)	[XXII]	$\frac{[\text{XXII}]}{[\text{XIX}]}$
1	0.171	0.121	0.7
1000	0.082	0.082	1.0
2000	0.040	0.052	1.2
2500	0.035	0.051	1.4

of the cyclic radical XVIIa originating from XVII has been observed, but such a reaction for XXIa is not known. If it does not exist, and recombination of the radical XVIIa accelerates with the increase of pressure then this would account for the marked increase of $[\text{XXII}]/[\text{XIX}]$.



Investigations showed [27, 28] that, with the application of high pressure, it is possible to regulate the ratio of cyclic and linear products in the homolytic addition of 1,3-oxazolidines to terminal olefins. Thus, during the reaction of *N*-propyl-1,3-oxazolidine (XVII) with hexene-1 in the presence of $t\text{-Bu}_2\text{O}_2$ at 423 K, when the pressure is raised from 1 to 10000 kg/cm² the rate of cyclic product formation (XXIII) increases 2-fold (Scheme VIII, Table VII) [27, 28].

With the increase of pressure the decrease in rate of the monomolecular rearrangement of 1,3-oxaza-2-cyclopentyl



Scheme VIII

radical (XVIIa) means that its participation in the addition to hexene-1 increases. Simultaneously, the proportion of rearranged amidoalkyl radicals (XVIIb) participating in the formation of the linear addition product (XXIV) decreases [27, 28].

So much for a purely qualitative interpretation of the effect. However, if an attempt is made to interpret it from even a semiquantitative aspect, this explanation is open to

Table VII

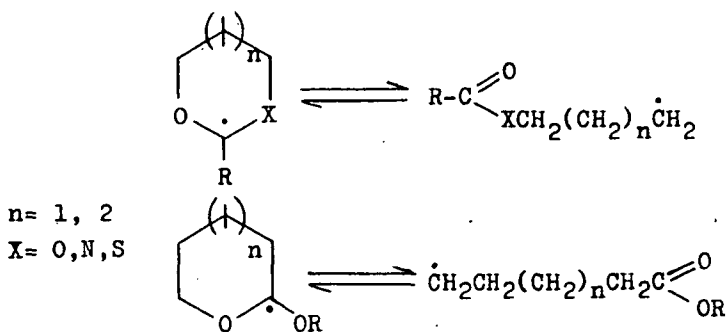
Influence of high pressure on the composition of products of radical addition of *N*-propyl-1,3-oxazolidine to hexene-1. [27, 28].

$T = 423 \text{ K}$ [hexene-1] = 0.5 mol/l, [*t*-Bu₂O₂] = 0.3 mol/l, [XVII] = 4 mol/l, solvent = chlorobenzene

Pressure (kg/cm ²)	$\frac{[\text{XXIV}]}{[\text{XXIII}]}$
1	1
1000	1.1
2500	1.2
5000	1.7
7500	1.8
10000	2.0

criticism in view of the modest nature of the effect. It seems necessary to take into account the influence of different recombination reactions on the yields of products XXIII and XXIV.

Analysis of the results permits the assumption that, in many cases of homolytic transformation of 1,3-oxaheterocycloalkanes under high pressure an equilibrium isomerization of cyclic radicals into linear acylheteroalkyl radicals takes place, with cyclization of the latter as a result of intramolecular addition to a C=O bond (Scheme IX).



Scheme IX

With the increase of pressure, the equilibrium is shifted to the left.

In general, the available data indicate that pressure fails to stimulate the homolytic transformation of acetals and their heteroanalogues, though it substantially influences the rates of the separate stages and changes the directions of the reactions noticeably.

For the decay of peroxides and nitrogen compounds ΔV_{-d}^{\ddagger} is accepted as equal to 3-5 cm³/mol [3]. In accordance with data on *t*-Bu₂O₂ decay in different acetals and their heteroanalogues and Eq. (5), in all solvents studied ΔV_{-f}^{\ddagger} has a positive value varying in the wide range 5-25 cm³/mol (Table VIII). Thus the radical fraction yielded by the "cell"

Table VIII

Volumetric effects of decay activation of *t*-Bu₂O₂ in different solvents at 403 K.

S o l v e n t	$\frac{V_{-f}^{\ddagger}}{-p}$ (cm ³ /mol)
2-isopropyl-1,3-dioxolane	10
2-propoxytetrahydropyran	11
4-methyl-1,3-dioxane	12
2-propyl-1,3-oxazolidine	13
1,1-diisobutoxyalkanes	12
<i>N</i> -propyl-2-ethyl-1,3-oxazolidine	15
2-isopropoxytetrahydropyran	17
2-methoxytetrahydropyran	19
2-cyclohexyloxytetrahydropyran	29

decreases substantially with the increase of pressure in some solvents. Certain considerations [3] suggest that, for *t*-Bu₂O₂ decay in all the solvents studied, recombination of *t*-BuO· in the "cage" takes place. The nature of the solvent has a substantial influence on the radical fraction yielded by the "cage". This may be closely connected with the different viscosity increases of the solvents under pressure and with the influence of solvent structure on the pressure-dependence of the recombination rate.

References

- [1] Gonikberg, M. G. : Chemical Balance and Rate of Reactions Under High Pressure. Khimiya, Moscow, 1969.
- [2] Isaac, N. S.: Liquid Phase High Pressure Chemistry. Wiley, 1980.
- [3] Zhulin, V. M.: Rev. Phys. Chem. Jpn., 50, 217 (1980).
- [4] Zhulin, V. M., S. I. Volchek: Khim. Geterotsikl. Soedin. 1979, 1443.
- [5] El'yanov, B. S., E. M. Vasilvitskaya: Rev. Phys. Chem. Jpn. 50, 169 (1980).
- [6] Rakhmankulov, D. L., S. S. Zlotskii: Khim. Geterotsikl. Soedin. 1977, 1011.
- [7] Kuhn, L. P., C. Wellmann: J. Org. Chem. 22, 774 (1957).
- [8] Huyser, E. S., D. T. Wang: J. Org. Chem. 29, 2720 (1969).
- [9] Imashev, U. B., S. S. Glukhova, S. M. Kalashnikov, S. S. Zlotskii, D. L. Rakhmankulov, Ya. M. Paushkin: Dokl. Akad. Nauk SSSR 237, 598 (1977).
- [10] Zorin, V. V., F. N. Latypova, B. V. Unkovsky, D. L. Rakhmankulov, S. S. Zlotskii: Zhur. Prikl. Khim. 49, 2681 (1976).
- [11] Latypova, F. N., V. V. Zorin, S. S. Zlotskii, D. L. Rakhmankulov, B. V. Unkovskii: Zhur. Org. Khim. 12, 1369 (1976).
- [12] Lapshova, A. A., V. V. Zorin, S. S. Zlotskii, R. A. Karakhanov, D. L. Rakhmankulov: Zhur. Org. Khim. 16, 365 (1980).
- [13] Zorin, V. V., S. S. Zlotskii, A. I. Gren', D. L. Rakhmankulov: Zhur. Org. Khim. 14, 1997 (1978).
- [14] Botnikov, M. Ya., S. S. Zlotskii, V. V. Zorin, E. Kh. Kravetz, V. M. Zhulin, D. L. Rakhmankulov: Izv. Akad. Nauk SSSR, Ser. Khim. 1977, 690.
- [15] Zorin, V. V.: Thesis, Ufa, 1977.
- [16] Kravetz, E. Kh., S. S. Zlotskii, V. S. Martem'yanov, D. L. Rakhmankulov: Zhur. Org. Khim. 12, 913 (1976).
- [17] Zelechonok, Yu. B., V. V. Zorin, S. S. Zlotskii, D. L. Rakhmankulov: Zhur. Org. Khim. 22, 863 (1986).

- [18] Zhulin, V. M., I. Kh. Milyavskaya: Izv. Akad. Nauk SSSR, Ser. Khim. 1974, 1487.
- [19] Gamagisky, T. G.: Tetrahedron Lett. 1971, 2795.
- [20] Pastushenko, E. V.: Thesis, Ufa, 1978.
- [21] Pastushenko, E. V., S. S. Zlotskii, M. Ya. Botnikov, V. M. Zhulin, D. L. Rakhmankulov: Zhur. Prikl. Khim. 52, 453 (1979).
- [22] Pastushenko, E. V., S. S. Zlotskii, D. L. Rakhmankulov: Khim. Geterosikl. Soedin. 1977, 456.
- [23] Imashev, U. B., V. V. Zorin, S. M. Kalashnikov, S. S. Zlotskii, V. M. Zhulin, D. L. Rakhmankulov: Dokl. Akad. Nauk SSSR, 242, 140 (1978).
- [24] Kalashnikov, S. M.: Thesis, Ufa, 1979.
- [25] Zhulin, V. M., B. I. Rubinstein: Izv. Akad. Nauk SSSR, Ser. Khim., 1976, 2201.
- [26] Lapshova, A. A., G. A. Stashina, V. V. Zorin, S. S. Zlotskii, V. M. Zhulin, D. L. Rakhmankulov: Zhur. Org. Khim. 16, 1251 (1980).
- [27] Lapshova, A. A.: Thesis, Ufa, 1980.
- [28] Lapshova, A. A., V. V. Zorin, S. S. Zlotskii, G. A. Stashina, V. M. Zhulin, D. L. Rakhmankulov: Zhur. Org. Khim. 17, 843 (1981).

РАДИКАЛЬНЫЕ ПРЕВРАЩЕНИЯ АЦЕТАЛЕЙ И ИХ АНАЛОГОВ В
ЖИДКОЙ ФАЗЕ ПРОИСХОДЯЩИХ ПОД ВЫСОКИМ ДАВЛЕНИЕМ

В.М. Жулин, В.В. Зорин, С.С. Злотский,
Д.Л. Рахманкулов, М. Барток и А. Молнар

Сопоставлены и проанализированы результаты жидкофазных гомолитических превращений циклических, линейно-циклических и линейных ацеталей и их N- и S-аналогов, происходящих под высоким давлением.

RHEOLOGIC PROPERTIES OF POLYELECTROLYTES AT LIQUID/LIQUID
INTERFACES

I. THE EFFECTS OF SURFACE-ACTIVE SUBSTANCES ON POLYELECTROLYTIC
ADSORPTIVE LAYERS

by

I.B. Musabekov and K.K. Ibraev

Kirov Kazakh State University, Alma-Ata, U.S.S.R.

(Received 12 December 1986)

Viscosity and strength of adsorption of layers of polyelectrolytes - poly(acrylic acid) (PAA), poly(methacrylic acid) (PMAA), polyethyleneimine (PEI) - on the boundary of their aqueous solutions with cationic (octadecylamine (ODA)) and anionic (stearic acid (HSt)) surface-active substances (SAS) dissolved in benzene. Associations of oppositely charged polyelectrolytes and SAS (PAA-ODA, PMAA-ODA, PEI-HSt) have the most structure-forming properties at interfaces.

Synthetic polyelectrolytes (SPE) are widely used in foam and emulsion stabilization. This is connected with their ability to accumulate in interfacial layers and form concentrated protective films. A very perspective trend in this field is SPE interfacial adsorptive layer (IFAL) modification by means of surface active substances (SAS).

The aim of the present work is to study the effects of the oil-soluble SAS stearic acid (HSt) and octadecylamine (ODA) on the interfacial shear viscosity of the IFAL SPE poly-methacrylic acid (PMAA), polyethyleneimine (PEI) and polyethyleneglycol (PEG). The methods of production and preparation of PMAA for work and the purification of the SAS are described in /1-3/. The branched PEI was kindly supplied by P.A. Gembitsky PEG produced by Schuchardt was used without preliminary purification. C.d.a. benzene was distilled twice (n_D^{20} 1.5006). The interfacial shear viscosity (η^s) was measured at 293 K by the method of Trapesnikov /4/ and was calculated via the formula:

$$\eta^{\sigma} = 2 K M (\lambda/T - \lambda_{\omega}/T_{\omega}) \quad (1)$$

where M is the effective value of the inertial moment of the suspension system in water, kg m^2 ; λ and λ_{ω} are the decrements of the disk vibration damping in the tested solution and in distilled water; and T and T_{ω} are the disk vibration periods in the tested solution and in distilled water, s.

$$K = (4\pi)^{-1} (1/R_1^2 - 1/R_2^2) \quad (2)$$

where R_2 is the internal radius of the cell immersed in the tested liquid, m; and R_1 is the glass disk radius, m. A 15 mm radius disk, a 50 mm diameter cell and tungsten filaments 0.53 m long and 0.05-0.14 mm wide were used in the study.

Figure 1 illustrates the kinetics of η^{σ} change at the aqueous PMAA and PEG solution/pure benzene and ODA benzene solution interfaces.

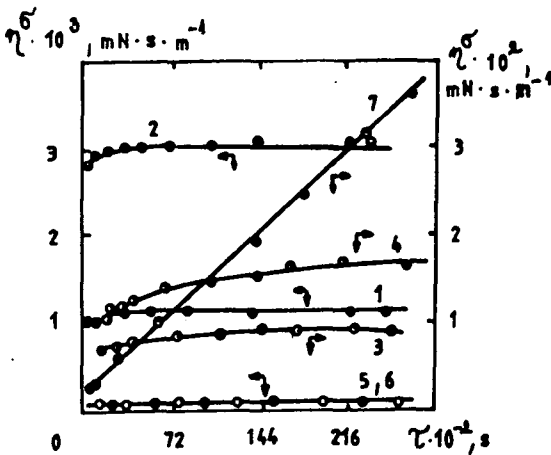
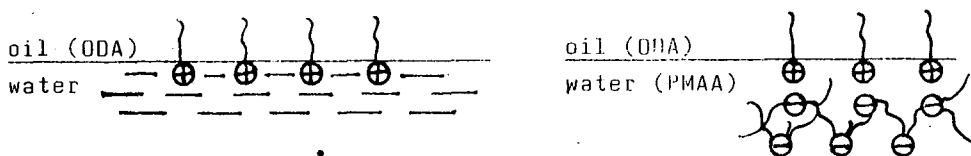


Fig. 1. Kinetics of η^{σ} change on the boundary of aqueous PEI (1,2) or PMAA (3,4,7) solutions with benzene (1,4), or with a $7.4 \cdot 10^{-4} \text{ mol dm}^{-3}$ ODA

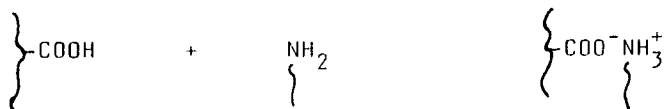
solution in benzene (7), and of water with $1 \cdot 10^{-3} \text{ mol dm}^{-3}$ ODA solution in benzene (5) or $7.04 \cdot 10^{-4} \text{ mol dm}^{-3}$ HSt solution in benzene (6). Concentrations of SPE (in mol dm^{-3}): PEI $2.28 \cdot 10^{-3}$ (1), $2.28 \cdot 10^{-2}$ (2); PMAA $4.7 \cdot 10^{-4}$ (3,5), $17.9 \cdot 10^{-4}$ (4).

That for the ODA benzene solution IFAL ζ^{σ} versus distilled water is also shown. It can be seen from the Figure that in the tested concentration interval ODA does not form adsorptive layers with noticeable viscosity and the absolute values of ζ^{σ} are within the limits of experimental error. Similar data are obtained with HSt. The PEI adsorptive layer viscosity is also small, though an insignificant increase in ζ^{σ} is observed with rise of the polyelectrolyte concentration. On the other hand, the equilibrium value of ζ^{σ} in PEI solutions is obtained rather rapidly, which may be connected with the weak adsorption of PEI due to its small chain difility. In contrast the equilibrium value ζ^{σ} in a PMAA solution is obtained after a long response time (2-8 hours), most likely because of delayed macromolecule diffusion to the interfacial surface in the dilute solutions and their slow denaturation in IFAL /5/ formed from concentrated solutions.

When an aqueous PMAA solution comes into contact with an ODA benzene solution, an abrupt rise in ζ^{σ} is observed, change in ζ^{σ} taking place over a long time period (Fig. 1, curve 7). The absolute value of ζ^{σ} is much larger than the summed value of ζ^{σ} for PMAA at the pure benzene - ODA benzene solution/water interface. In other words, a synergetic effect is observed in the ζ^{σ} increase, which may be connected with PMAA+ODA complexation at the interface. This process can be represented schematically in the following way:



The ODA positive charge probably arises as a result of amino group protonation by the polyacid carboxylic group proton:



The slow change in ζ^{σ} may be a result of the delayed macromolecule conformation equilibrium in IFAL.

Figure 2 gives η^{σ}/C_{SPE} isotherms for PEG, PMAA and PEI/HSt mixtures. The nonionic polymer PEG having an average molecular mass of $4 \cdot 10^4$ is weakly adsorbed at the water/benzene interface and forms adsorptive layers with low η^{σ} values. The IFAL viscosity gradually rises with PMAA

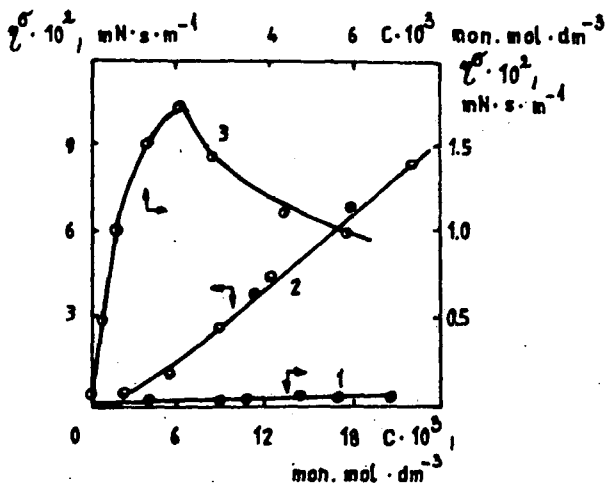


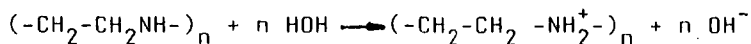
Fig. 2. η^{σ} isotherms of aqueous solutions of PEG (1), PEI (2) and PMAA (3) on the boundary of contact with benzene (1,3) and $7.04 \cdot 10^{-4} \text{ mol dm}^{-3}$ HSt solution in benzene (2).

concentration increase, passing through a maximum; this may be connected with the difficulty of macromolecule adsorption from concentrated solutions due to structure-forming /6/.

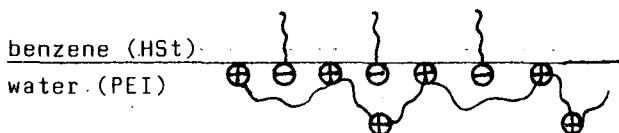
When an aqueous PEI solution comes into contact with an HSt solution, a linear rise in η^{σ} is observed, accompanied by a high-molecular component concentration increase.

The introduction of oil-soluble SAS into the nonpolar phase does not essentially affect the η^{σ} of an aqueous PEG solution. The absolute value of η^{σ} greatly exceeds the IFAL viscosity of the separate components for the aqueous PEI solution/HSt benzene solution system. As in the above-mentioned PMAA/DDA system, the considerable rise in η^{σ} is connected

with the formation of a PEI/HSt association in the interfacial adsorptive layer. The HSt concentration at the interface leads to the appearance of the negative charge at the benzene surface. On the other hand, PEI receives positive charge as a result of interaction with water:



Thus, a PEI/HSt electrostatic interaction in the adsorptive layer becomes possible and is expressed by the following scheme:



The interaction of the SPE and SAS functional groups stimulates stronger hydrophobic segment interaction, and also leads to PEI chain fixation at the interface. All this causes a sharp viscosity increase for the PEI/HSt associations in IFAL. The increase in η^6 at the aqueous polyelectrolyte solution/SAS benzene solution interface, the two compounds being oppositely charged, is enhanced by the concentration increase of both components, irrespective of their nature. Thus, an increase of the initial PEI concentration in its aqueous solution is accompanied by an increase in the rate of rise of η^6 at the interface of HSt benzene solutions of increasing concentration /Fig. 3/. A similar effect is observed at the aqueous PMAA solution/ODA benzene solution interface (Fig. 4).

In both cases, however, the introduction into the nonpolar phase of SAS charged similarly to SPE leads to a substantial decrease in η^6 (Fig. 3, curve 4; Fig. 4, curve 4). This is not surprising, for the accumulation of SAS charged similarly to SPE at the interface leads to a decreased polymeric ion adsorption, in accordance with the SPE adsorption theory relating to charged surfaces /7/.

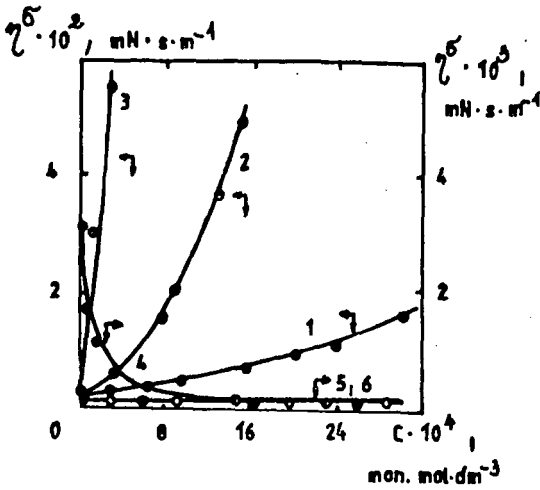


Fig. 3. ζ^{σ} isotherms of benzene solutions of HSt (1-3,6) and ODA (4,5) on the boundary of contact with water (5,6) and aqueous solutions of PEI (1-4).

Concentration of PEI ($\text{mol} \cdot \text{dm}^{-3}$): $2.28 \cdot 10^{-3}$ (1), $6.84 \cdot 10^{-3}$ (2) $2.28 \cdot 10^{-2}$ (3,4).

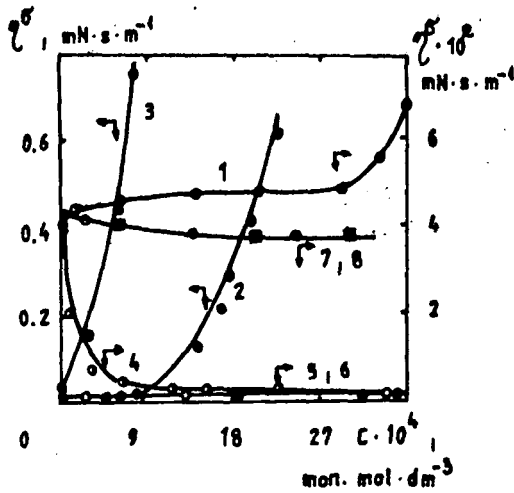


Fig. 4. ζ^{σ} isotherms of benzene solutions of ODA (1-3,5,7) and HSt (4,6,8) on the boundary of contact with water (5,6) and aqueous solutions of PMAA (1-4) and PEG (7,8). Concentration of SPE ($\text{mol} \cdot \text{dm}^{-3}$): PMAA $3.5 \cdot 10^{-4}$ (1), $4.7 \cdot 10^{-4}$ (2), $17.9 \cdot 10^{-4}$ (3,4); PEG $1.6 \cdot 10^{-2}$.

The SAS have practically no influence on the IFAL ²⁶ of an aqueous PEG solution. (Fig. 4, curve 7).

Conclusion: the rheologic properties of IFAL polyelectrolytes at a water/hydrocarbon interface can be regulated by means of SAS introduced into the nonpolar phase.

References

- /1/ Aidarova, S.B., K.B. Musabekov: Kolloidn. Zh. 41, 117 (1979)
- /2/ Wiederhorn, N.M., A.R. Brown: J. Polym. Sci., 8, 651 (1952)
- /3/ Musabekov, K.B., K.K. Ibraev: V knige: Fiziko—chimicheskie issledovaniya v rastvorach, Alma-Ata, 123 (1982)
- /4/ Vins, V.G., A.A. Trapeznikov: Dokl. Akad. Nauk (USSR), 248 1352 (1979)
- /5/ Tanchuk, Yu.V., G.S. Pop: Kolloidn. Zh. 40, 1209 (1978)
- /6/ Lipatov, Yu.S., L.M. Sergeeva: Adsorptsiya polimerov, Kiev, Naukova dumka, 1972
- /7/ Kuzkin, S.V., V.P. Nebera: Sinteticheskie flokulyanty v protsesakh obezvozhivania, Moskva, Gostekhizdat, 1963

РЕОЛОГИЧЕСКИЕ СВОЙСТВА ПОЛИЭЛЕКТРОЛИТОВ НА ГРАНИЦЕ ЖИДКОСТЬ—ЖИДКОСТЬ. I. ВЛИЯНИЕ ПОВЕРХНОСТНО—АКТИВНЫХ ВЕЩЕСТВ НА АДсорбЦИОННЫЕ СЛОИ ПОЛИЭЛЕКТРОЛИТОВ.

К.Б. Мусабеков, К.К. Ибраев

Изучены вязкость и прочность адсорбционных слоев полиэлектролитов /полиметакриловой (РММА) кислоты, полиэтиленимина (PEI)/ на границе их водных растворов с растворенным в бензоле катионным /октадециламин (ОДА)/ или анионным /стеариновая кислота (HSt)/ поверхностно—активным веществом (SAS). Наибольшими структурообразующими свойствами в межфазных слоях обладают ассоциаты противоположно заряженных полиэлектролитов и SAS: РММА—ОДА, PEI—HSt.

INDEX

I.Gyémánt and Zs.Varga: 1s Core-Level Shifts in Al-Clusters of Increasing Size	3
Gy.Papp, P.Boguslawski and A.Baldereschi: Electron Energy of Hexagonal Site Self-Interstitial Impurity in Si	9
J.Császár: UV and ^1H NMR Spectra and Conformations of Substituted N-Benzylideneanilines	17
P.Nagy and R.Herzfeld: Study of the Solvent Effect in the Amine Exchange of Schiff Bases V. Connection between the Rate Constant and the Parameters E_T^N and B_{KT} of the Solvent Mixtures Applied	33
V.M.Zhulin, V.V.Zorin, S.S.Zlotskii, D.L.Rakhmankulov, M.Bartók and Á.Molnár: Liquid-Phase Radical Reactions of Acetals and their Analogues at high Pressure	45
K.B.Musabekov and K.K.Ibraev: Rheologic Properties of Polyelectrolytes at Liquid/Liquid Interfaces I. The Effects of Surface Active Substances on Polyelectrolytic Absorptive Layers	71





F.k.: Dr. Bartók Mihály a TTK dékánja

Készült a JATE Sokszorosító Üzemében
Engedélyszám: 5/87 Méret/E/5
Példányszám: 450 F.v.: Lengyel Gábor